

Remarks

Claims 37-40 have been amended. Claims 1-36, 41-57 and 59-60 have been previously cancelled. By entry of this amendment, claims 37-40, 58 and 61 are pending.

Rejections under 35 U.S.C. §112, first paragraph (written description)

Claims 37-39, 40, 58 and 61 have been rejected under 35 U.S.C. §112 as lacking written description. Applicants traverse the rejection as applied to the claims as amended.

The Examiner asserts that the standard for written description requires sufficient disclosure of structural and functional characteristics coupled with a correlation between the structural and functional characteristics. The legal standard for written description also permits claims to a genus provided that a representative number of species is described to support the genus (*See Amgen, Inc. v. Hoechst Marion Roussel, Inc. and Transkaryotic Therapies, Inc.*, 314 F.3d 1313 (Fed. Cir. 2003)).

Claims 37-39 recite that the DOI-1 polypeptide is encoded by SEQ ID NO:1 and functional variants and alleles thereof. The originally filed application states that the 'terms "variants" and "alleles" means that they are derived from the sequences given in the figures and have the same function as those'. (Page 2, lines 12-13).

Structural features of the DOI-1 polypeptide are described in the specification and portrayed in Figure 1. DOI-1 polypeptides comprise a glutamine rich region, an acidic region, NLS, zinc finger region and basic region. The NLS regions specifically confer the function of the protein to translocate to the nucleus at the onset of apoptosis. Mutant peptides lacking the NLS domains lose their function and do not translocate to the nucleus and thereby fail to cause apoptosis. (Garcia-Domingo et al. *Mol. Cell. Biol.* 2003, 23 pp 3216-25). Furthermore,

BEST AVAILABLE COPY

applicants have provided the sequences of the human and murine homologs (SEQ ID NO:3 and NO:4) which demonstrate a remarkable conservation between species. In view of this high degree of conservation, one of ordinary skill would be readily able to identify sequences containing the structures that would maintain DOI-1 function and then screen a reasonable number of sequences using the methods taught by the examples specification.

The Examiner asserts that Applicants have not provides specific functional activity of DOI-1 and therefore one of ordinary skill would be unable to readily screen for functional variants and alleles of DOI-1. Applicants respectfully disagree. The level of skill in the art is high and the specification teaches at page 2, lines 17-22 that DOI-1 plays a role in controlling apoptosis and also being useful for the treatment of a number of conditions. The function of DOI-1 in controlling apoptosis is further described in the specification in Examples 5-7 of the specification. The Examiner concurs that the DOI-1 protein causes cells to undergo apoptosis. Specifically, DOI-1 is expressed during murine limb development and plays a role in the patterning of postero-distal limb and digit development. This function is verified by Applicant's later published article (Garcia-Domingo et al, 2003). The pathways of apoptosis are remarkably conserved *in vitro* and *in vivo* and a wide range of methods and assays were known at the time of filing to study apoptosis. The effect of DOI-1 on apoptosis provides the skilled artisan with adequate function to allow identification of DOI-1 polypeptides and functional variants thereof.

Assays for apoptosis were commercially available and widely used at the time of filing. It would have been well within the purview of the skilled artisan, using the teachings of the specification and commercially available assays such as TUNEL to identify variants of DOI-1 comprising the regions depicted in Figure 1 and readily screen them for induction of apoptosis. Applicants have sufficiently described the genus of DOI-1 polypeptides complete with structural

features, function and a correlation therebetween. As such, withdrawal of the rejection is respectfully requested.

Rejections under 35 U.S.C. §112, first paragraph (enablement)

Claims 58 and 61 have been rejected under 35 U.S.C. §112 for failing to comply with the enablement requirement. Applicants traverse the rejection as applied to the claims as amended.

Claims 58 and 61 are directed to an isolated polypeptide of SEQ ID NO:3 or SEQ ID NO:4 for use as a medicament.

The Examiner asserts that the skilled artisan would be unable to extrapolate the teachings of the specification which provide a viral expression vector to express DOI-1, to the claims which provide a formulation of a DOI-1 protein for administration.

The *in vitro* experiments are representative of the *in vivo* situation and (b) the skilled man would readily be able to create a pharmaceutical composition comprising SEQ ID NO:3 or NO:4 without undue inventive or experimental effort. The polypeptides of SEQ ID NO:3 and NO:4 both possess the NLS and would be translocated to the nucleus to control apoptosis. The specification confirms this action. There is no reason to believe that these proteins would have different actions because they are expressed versus administered. In fact, the claimed composition could be manufactured using the same retroviral vector disclosed in the specification for expression of the polypeptide product.

The apoptotic pathway is studied almost exclusively *in vitro*, because it is preserved at the cellular level rather than at the level of the organism. Nonetheless, this pathway is essential for life, and therefore conserved in all cells of the individual. The effects of DIO-1 on apoptosis

will therefore be the same in cultured cells and cells in the organism, and the *in vitro* data presented are thus representative of the *in vitro* situation. Data presented in Applicants own article confirm that DIO-1 acts directly on the regulation of caspase levels in the cell from inside the nucleus (Garcia-Domingo et al., 2003). A pharmaceutical formulation as described in claims 58 and 61 has been tested and found effective in a controlled *in vivo* experiment (Figures 4 and 5 in the original application, reproduced from the reference: "DIO-1 is a gene involved in onset of apoptosis, whose misexpression disrupts limb development", Garcia-Domingo et al., PNAS USA 1999, 96 pp 7992-7997).

Although these papers were published after the filing date of the present application, they report work carried out before the filing date and therefore demonstrate that the skilled man was able to carry out such procedures at the relevant time. Applicants have readily enabled the skilled artisan to make the claimed compositions and respectfully request withdrawal of this rejection.

Rejections under 35 U.S.C. §102

Claims 37-39 and 61 have been rejected under 35 U.S.C. §102(b) as being anticipated by Nagase et al. (*DNA Research* 1997; 4(2):pp141-150). Applicants traverse the rejection as applied to the claims as amended.

The original sequence published by Nagase et al. discloses only part of the complete DIO-1 sequence as shown by the enclosed alignments and the alignment provided by the Examiner. Components essential for DIO-1 function, such as the nuclear localization signal (NLS), are not present in the original sequence presented by Nagase et al. Proof for this novel identification of an essential part of DIO-1 is provided (Garcia-Domingo et al., 2003). In addition, Nagase et al. do not assign any function to the sequence retrieved.

The Examiner states that there is no *prima facie* reason to believe that the Nagase sequence would fail to have the same function as DOI-1 because such functions and actions would be inherent to the polypeptide. The Examiner requests that objective evidence to the contrary is required to demonstrate that the Nagase sequence is not a functional DOI-1 polypeptide variant. The Nagase sequence is missing 200 amino acid residues of the DOI-1 protein and fails to include an NLS sequence as shown by the enclosed alignment diagrams (shaded underlined). The NLS domain is an essential structure in the DOI-1 polypeptide which permits nuclear localization at the onset of apoptosis. (specification page 7, lines 30-35). The enclosed article by Garcia-Domingo et al. (2003) demonstrates that a DOI-1 deletion mutant lacking the NLS domain is non-functional. Therefore, the Nagase sequence also lacking the NLS domain would be non-functional and would therefore not constitute a DOI-1 polypeptide or functional variant nor would Nagase anticipate the claims.

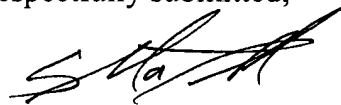
For a prior art reference to anticipate a claim, the prior art reference must disclose all elements of the claim and also be an enabling disclosure. Nagase gives no indication that if expressed, their nucleotide sequences would provide a functional DIO-1 protein. Applicants provide objective evidence that the Nagase sequence is non-functional and therefore respectfully request withdrawal of this rejection.

Conclusion

Applicants submit that the pending claims define novel and patentable subject matter and provide a complete response to the Office Action. Accordingly, Applicants respectfully request allowance of these claims. No additional fees are believed due, however, the Commissioner is hereby authorized to charge any deficiencies which may be required, or credit any overpayment, to Deposit Account Number 11-0855.

Early and favorable consideration is earnestly solicited. If the Examiner believes any informalities remain in the application that can be resolved by telephone interview, a telephone call to the undersigned attorney is earnestly solicited.

Respectfully submitted,



Stephen C. MacDonald, Ph.D.
Reg. No.- L0063

KILPATRICK STOCKTON LLP
1100 Peachtree Street
Suite 2800
Atlanta, Georgia 30309-4530
Tel. (404) 815-6500
Docket No : 46309-253995

DIO-1 is a gene involved in onset of apoptosis *in vitro*, whose misexpression disrupts limb development

(transcription factors/interdigital webs)

DAVID GARCÍA-DOMINGO*, ESTHER LEONARDO*, ALF GRANDIEN*†, PEDRO MARTÍNEZ*, JUAN PABLO ALBAR*, JUAN CARLOS IZPISÚA-BELMONTE‡, AND CARLOS MARTÍNEZ-A*§

*Department of Immunology and Oncology, Centro Nacional de Biotecnología, Universidad Autónoma, Campus de Cantoblanco, E-28049 Madrid, Spain; †Department of Immunology, Stockholm University, Stockholm, Sweden; and ‡The Salk Institute, 10010 North Torrey Pines Road, La Jolla, CA 92037

Communicated by A. García-Bellido, Autonomous University of Madrid, Madrid, Spain, April 23, 1999 (received for review March 3, 1999)

ABSTRACT The *DIO-1* (death inducer-oblierator-1) gene, identified by differential display PCR in pre-B WOL-1 cells undergoing apoptosis, encodes a putative transcription factor whose protein has two Zn finger motifs, nuclear localization signals, and transcriptional activation domains, expressed in the limb interdigitating webs during development. When overexpressed, *DIO-1* translocates to the nucleus and activates apoptosis *in vitro*. Nuclear translocation as well as induction of apoptosis are lost after deletion of the nuclear localization sequences. *DIO-1* apoptotic induction is prevented by caspase inhibitors and Bcl-2 overexpression. The *in vivo* role of *DIO-1* was studied by misexpressing *DIO-1* during chicken limb development. The most frequently observed phenotype was an arrest in limb outgrowth, an effect that correlates with the inhibition of mesodermal and ectodermal genes involved in this process. Our data demonstrate the ability of *DIO-1* to trigger apoptotic processes *in vitro* and suggest a role for this gene in cell death during development.

Apoptosis is a major form of cell death, characterized morphologically by chromatin condensation, nuclear disruption, and formation of cytosol containing apoptotic bodies. It is an efficient mechanism for eliminating unwanted cells and is of central importance for development and homeostasis in metazoan animals (1). Many different signals within or from outside the cell have been shown to influence the decision between life and death (2). Most are controlled through triggering of specific receptors, which leads to activation of specific mediators; they may then act to suppress or promote activation of the death program. It is hence not surprising that initiation of apoptosis is precisely regulated.

A common meeting point for cell death signals is the cytoplasm, where the caspases exert their function and are blocked by their inhibitors (3–6). Very little is known as to how these signals are transmitted to the nucleus. A caspase-activated DNase (CAD) and its inhibitor (ICAD) have recently been identified in the cytoplasmic fraction of a mouse lymphoma cell line. Caspase pathway activation by different stimuli cleaves ICAD, allowing CAD to enter the nucleus and degrade chromosomal DNA (7, 8). In addition to the caspases, inducible gene products also appear to be required for apoptotic death in some cell types (9). Evidence for this was derived from experiments in which cell death could be suppressed by the inhibition of RNA or protein synthesis in cells that should otherwise die (10), suggesting that gene transcription and RNA translation are required for death to occur in these cells. Indeed, transcriptional activation of specific genes is absolutely required for physiological apoptosis in both insect and verte-

brate embryos (10, 11). Several transcriptional regulators are known to control apoptosis, among which p53 (12), Nur77 (13), the glucocorticoid receptor (14), STAT1 (15), c-myc (12, 16), c-jun (17), and NF- κ B (18) have been identified to date.

Much of the natural cell death that occurs during insect and vertebrate development appears to be mediated by the transcriptional activation of killer genes. Although no such genes have yet been identified in vertebrates, recent studies in the fly *Drosophila melanogaster* have uncovered three components of the genetic program controlling programmed cell death (PCD), *hid*, *grim*, and *reaper*, whose transcriptional activation precedes, induces, and is necessary for PCD by apoptosis (19–21). The three genes map to a single genetic complex and function as death switches that are regulated at the level of transcription. Their ectopic activation triggers apoptosis in otherwise viable cells, and their inactivation prevents apoptosis of cells that would normally undergo PCD. We and others have recently demonstrated that the expression of one of these genes, *grim*, activates apoptosis in mammalian cells, implying conservation during metazoan evolution of both the gene and the mechanisms required to trigger cell death (9).

The developing limb is perhaps one of the best-suited model systems for the study of this process, because fine tuning is required between cell proliferation and cell apoptosis to allow proper limb modeling, a process subject to intervention without endangering embryo viability. Whilst much has recently been learned regarding factors involved in cell proliferation, less is known about the mechanisms implicated in programmed cell death during development. It has recently been shown that inhibition of NF- κ B translocation by viral overexpression of a transdominant-negative I κ B leads to perturbation of limb outgrowth (22). We have now tested *in vivo* the effect of a, to our knowledge, novel gene, *DIO-1* (death inducer-oblierator-1), identified by differential display PCR in pre-B cells undergoing apoptosis. Its mRNA and protein are present at very low levels in the cytoplasm. Once an appropriate apoptotic signal is detected, the protein translocates to the nucleus and up-regulation is observed at both transcript and protein levels. When overexpressed, it induces apoptosis in cell lines growing *in vitro*, which is prevented by blocking caspase activity. The protein encoded, DIO-1, is expressed in the limb interdigitating membranes during development. *DIO-1* expression in distal proliferating mesodermal cells of the developing chicken limb bud prevents limb outgrowth, an effect that correlates with inhibition of mesodermal and ectodermal genes involved in limb outgrowth. These data demonstrate the ability of *DIO-1* to trigger apoptotic processes *in vitro*, as well as the

Abbreviations: AER, apical ectodermal ridge; E2, 17 β -estradiol; NLS, nuclear localization signal.

Data deposition: The sequence reported in this paper has been deposited in the GenBank database (accession no. AJ238332).

§To whom reprint requests should be addressed. e-mail cmartinez@cnb.uam.es.

The publication costs of this article were defrayed in part by page charge payment. This article must therefore be hereby marked "advertisement" in accordance with 18 U.S.C. §1734 solely to indicate this fact.

PNAS is available online at www.pnas.org.

utility of limb development as a model system to characterize genes involved in apoptosis.

MATERIALS AND METHODS

Cloning of *DIO-1*. Differential display experiments were performed by using an RNAmapping kit (GenHunter, Brookline, MA) according to the manufacturer's specifications. Briefly, 200 ng of total cytoplasmic RNA (after DNase treatment with the MessageClean Kit; GenHunter) isolated from WOL-1 cells at 0, 2, 4, and 8 h after IL-7 withdrawal were reverse transcribed with oligo(dT) primers ($T_{12}MN$) in the presence of Moloney murine leukemia virus reverse transcriptase. They were amplified with several combinations of 5' decamer arbitrary primers and the $T_{12}MN$ used for reverse transcription in the presence of [^{35}S]dATP (1,200 Ci/mmol). Amplified products were resolved in an 8-M urea/6% polyacrylamide DNA sequencing gel and analyzed by autoradiography. Bands of interest were isolated, reamplified, cloned in the pCR-Script SK(+) vector (Stratagene), and used for Northern analysis and sequencing. *DIO-1* cDNA was obtained from WOL-1 cDNA by 5' rapid amplification of cDNA ends (RACE) by using a Marathon cDNA Amplification Kit (CLONTECH), with the 3' primer L282 (5'-AGGTGTACCTTGACAGCAGT-GAAAC-3'). The resulting 2.6-kbp band was excised from the gel and cloned in the TA-type vector pGEM-T (Promega). Resulting clones were sequence analyzed for orientation, and the oriented sense with respect to the T7 promoter was called *DIO-1pGEM-T*. To confirm the ORF sequence obtained, a cDNA library from mouse brain cloned in λ ZAP II (Stratagene) was screened by probing with the RACE clone; the same probe was used to screen a human fetal kidney cDNA library (CLONTECH) from which the human *DIO-1* homologue was cloned.

Cells and Transfections. WOL-1 cells were derived from adult BALB/c mouse bone marrow. WOL-1 is an untransformed IL-7-dependent stroma cell-independent pre-B1 cell line, capable of reconstituting irradiated severe combined immunodeficient mice. Cells were cultured in Iscove's modified Dulbecco's medium supplemented with penicillin (100 units/ml)/streptomycin (100 μ g/ml)/1 mM sodium pyruvate/nonessential amino acids/50 μ M 2-mercaptoethanol/2 mM L-glutamine/10% FCS/IL-7 (3% supernatant from a murine IL-7-producing cell line). The Ba/F3 and FL5.12 cell lines were maintained in RPMI medium 1640 with 10% FCS and 5% supernatant of a murine IL-3-producing cell line, whereas A20 and WEHI-231 grew in the same medium without IL-3. The FL5.12hBcl-2 stable cell line was cultured in 1 mg/ml G-418 (Calbiochem). MEF(10.1)Val5MycER cells were cultured at 39°C in phenol red-free DMEM containing 10% FCS. Where indicated, 1 μ M 17 β -estradiol (E2) was added to activate the MycER fusion protein after 24 h FCS starvation (12). WOL-1, A20, Ba/F3, and FL5.12 cell lines were cultured at 37°C, and all cell lines were maintained in a humidified atmosphere with 5% CO₂.

Transient DNA transfection was performed by electroporation. For each transfection, 2×10^6 log phase cells were collected by centrifugation and resuspended in 200 μ l of RPMI medium 1640 without FCS. After addition of 10 μ g of plasmid DNA (1 mg/ml), samples were gently shaken and electroporated in a 0.4-cm electrode gap gene pulser cuvette at 960 μ F and 320 V with a GenePulser (Bio-Rad). Samples were diluted with 6 ml of the same medium supplemented with 10% FCS and incubated at 37°C in a humidified atmosphere with 5% CO₂. Cells were analyzed for cell-cycle staining by FACS at 48 h after electroporation.

Northern Blot Analysis. Total cytoplasmic RNA was prepared as described (23). RNA (10 μ g) was Northern blotted by using a ^{32}P -labeled *DIO-1* riboprobe made by *DIO-1pGEM-T* digestion with *Bgl*II and *in vitro* transcribed from SP6 by using

the Riboprobe *In Vitro* Transcription System (Promega). Hybridization was performed in 50% formamide at 65°C; washes were in 0.1 \times SSC + 0.1% SDS at 80°C. Blots were exposed on Kodak X-Omat AR film at -70°C with two intensifying screens.

Antibody Production and Western Blot. We synthesized a peptide corresponding to amino acids 58–72 of murine *DIO-1* with an additional N-terminal cysteine (CSLRRSGRQPKRTERV); it was coupled to maleimide-activated keyhole limpet hemocyanin and the purified conjugate injected into New Zealand White rabbits. Polyclonal antibody was affinity purified on a peptide-thiopropyl Sepharose column. For Western blot, cells were collected at different times after IL-7 removal from culture medium; 5×10^5 cells were lysed with RIPA buffer (0.15 mM NaCl/0.05 mM Tris-HCl, pH 7.2/1% Triton X-100/1% sodium deoxycholate/0.1% SDS), and the total extract separated in 8% SDS/PAGE, transferred and incubated with the affinity-purified polyclonal anti-*DIO-1* antibody (1:100 dilution in TBS-1% nonfat dry milk). Protein-loading equivalence was confirmed by Ponceau S staining.

In Situ Hybridization and Histology. Whole-mount *in situ* hybridization was as described (24) with minor modifications (25). The *DIO-1* digoxigenin probe was made by *Bgl*II digestion of the *DIO-1pGEM-T* and transcription from the SP6 promoter. The probe used for *Lhx-2* (700 bp) encompasses the homeobox and the second LIM (*lin-11*, *Isl-1*, *mec-3*) domain. The remaining probes have been described elsewhere and include *Msx-1* (26), *Fgf-8* (27), and *NF- κ B* (22). To visualize cartilage, embryos were fixed in trichloroacetic acid after viral infection, stained with 0.1% alcian green, and dehydrated/cleared in methyl salicylate.

Virus Production and Injection Protocols. Chicken embryos (from MacIntyre Poultry, San Diego, CA, or SPAFAS, Preston, CT) were infected with a virus containing the *DIO-1* ORF. Virus preparation and injections were as previously described (28). After injection, embryos were incubated at 37°C and fixed at different time points for *in situ* hybridization or phenotypic analysis.

RESULTS

Isolation of *DIO-1* cDNA: Protein Structure and Sequence Relationships. To search for genes implicated in apoptosis, we used the differential display PCR (DDRT-PCR) technique (29) using mRNA obtained from the WOL-1 pre-B cell line as a target. WOL-1 was derived from BALB/c adult bone marrow; it grows exponentially in the presence of IL-7 and undergoes apoptosis on IL-7 withdrawal. The DDRT-PCR technique gave rise to several positive bands, 10 of which were initially identified as undergoing up- or down-regulation during apoptotic death and were therefore considered candidates for subsequent analysis. They were further amplified, sequenced, and compared with known gene sequences by using the National Center for Biotechnology Information BLAST program (30). Of these, one band (*DIO-1*) revealed that the nucleotide sequence was a gene that showed no significant identity to any known gene or translated products in the databases. To confirm the sequence obtained by rapid amplification of cDNA ends (RACE), a murine cDNA library was screened by using a labeled *DIO-1* probe. Five positive clones were identified and characterized by restriction mapping and sequencing. Analysis of the cDNA revealed inserts identical in sequence to the ORF cloned by RACE. The longest ORF corresponds to a 614-aa protein (Fig. 1A) and shows a Kozak consensus sequence before the ATG (considered as the +1 position) known to be crucial for initiation of translation (31). (It also comprises a putative nuclear localization signal (NLS) and transcriptional activation domain in the N-terminal region, two central Zn finger motifs, and a lysine-rich carboxyl terminus. Having analyzed the domains of the putative pro-

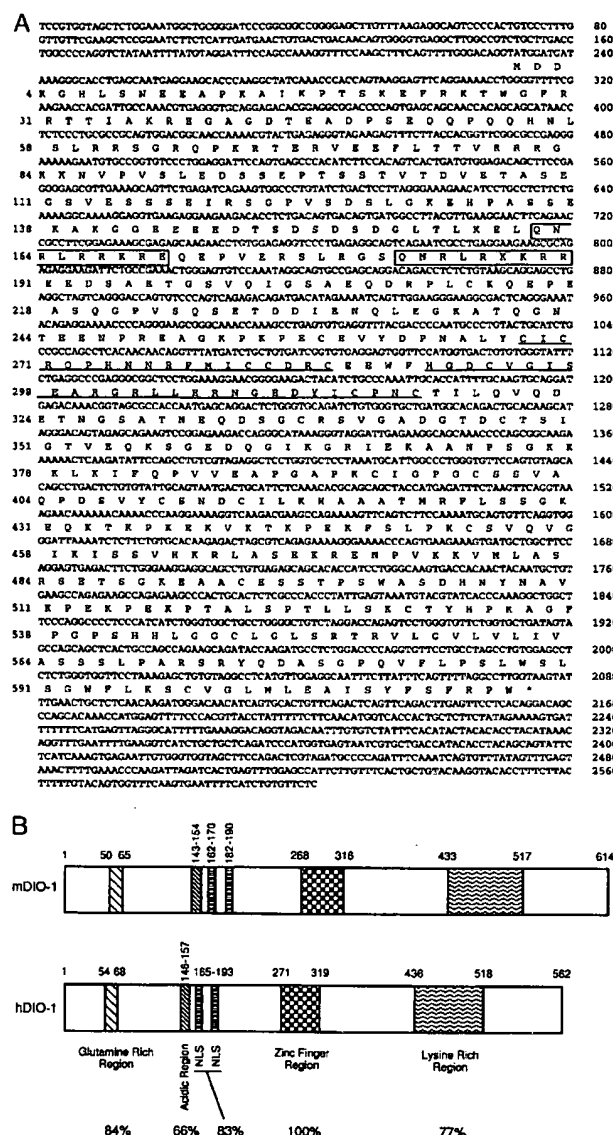


FIG. 1. Nucleotide and predicted amino acid sequences of murine and human *DIO-1*. (A) The bipartite NLS sequence is boxed, and the zinc finger motifs are underlined. (B) Schematic representation of the predicted ORF of murine and human *DIO-1*. The start and end positions of the amino acids defining the motifs are numbered above. Percentages indicate degree of identity between human and mouse for each domain. Overall similarity is 74%.

tein, we sought to determine their degree of conservation in closely related species to assess their function. A human cDNA library was screened by using the murine clone as probe; positive clones were sequenced and showed strong similarity to the murine gene in the ORF, with a high degree of structural and compositional conservation (Fig. 1B).

***DIO-1* Is Present in All Tissues and Its Levels Are Up-Regulated During Apoptosis.** To study *DIO-1* gene regulation during apoptosis, *DIO-1* expression pattern was examined by Northern blot analysis. Various tissues were analyzed to determine *DIO-1* transcript distribution, and two 9.5- and 5.4-Kb mRNA species were detected in all tissues tested (Fig. 2A). Southern blot analysis of genomic DNA showed that *DIO-1* is a single-copy gene in both mouse and human. RNA samples were isolated from several cell lines in exponential growth or undergoing apoptosis as a result of various experimental treatments. In the exponential growth phase, WOL-1 cells

express low levels of *DIO-1* mRNA, which increase after induction of apoptosis (Fig. 2B). *DIO-1* is up-regulated in IL-7-deprived cells or those treated with IFN- γ or dexamethasone, but not in cells treated with etoposide. UV irradiation, or in those undergoing p53-induced cell death (Fig. 2B). It is also up-regulated in anti-IgM-treated WEHI-231 cells. In MEF(10.1)Val5MycER cells, up-regulation is observed in the absence of serum after addition of E2, but not before or at 32°C (even in the presence of E2 or serum). Up-regulation of *DIO-1* mRNA levels in cells undergoing apoptosis was confirmed in Western blot by using a polyclonal anti-*DIO-1* antibody raised against a synthetic peptide comprising amino acids 58–72. In cell extracts derived from WOL-1 cells undergoing IL-7 deprivation-induced apoptosis, a 67-kDa band was up-regulated 2 hr after induction (Fig. 2C), but not after etoposide-induced cell death (data not shown). In all cases in which up-regulation of the *DIO-1* transcript or of the *DIO-1* protein itself was detected, there was a clear peak in the kinetic levels of *DIO-1* up-regulation before any signs of cell death were detectable.

***DIO-1*-Induced Apoptosis Is Inhibited by Bcl-2 and Z-VAD and Lost by Deletion of the NLS.** The role of *DIO-1* in the apoptotic process was evaluated by transient transfection of the gene into several cell lines and examination of cell death kinetics. Transfection of a *DIO-1* expression plasmid into Ba/F3 cells results in a dramatic loss of cell viability at 48 hr after transfection (Fig. 3). All cells displayed morphological alterations characteristic of apoptosis, becoming rounded, condensed, and finally dying. This effect was specific in that transfection of Ba/F3 with an empty vector had no effect on cell survival. To verify the generality of this observation, *DIO-1* constructs were transfected into A20 or FL5.12 cells (Fig. 3). In both cases, apoptosis was induced after kinetics similar to those observed for Ba/F3. Transfection into MEF(10.1)Val5MycER cells gave rise to apoptotic morphology as assessed by 4',6'-diamidino-2-phenylindole staining; using the *DIO-1*-specific antibody, we found that endogenous *DIO-1* is located in the cytoplasm of MEF(10.1)Val5MycER cells in exponential growth. When apoptosis is triggered in these cells by addition of E2 at 39°C in the absence of serum, *DIO-1* is translocated to the nucleus (not shown). This translocation appears to be critical for activation of the apoptotic pathway, as deletion of the NLS renders the *DIO-1* protein unable to translocate to the nucleus, thus impairing its ability to trigger apoptosis (Fig. 3). When *DIO-1* was transfected into stable FL5.12 cells overexpressing human Bcl-2, cells were resistant to apoptosis, showing that Bcl-2 coexpression inhibits *DIO-1* death-promoting activity, as has also been described for other systems (32). We also incubated *DIO-1*-transfected FL5.12 cells alone or in the presence of the caspase inhibitor Z-VAD-fmk. After 48-h expression in the presence of IL-3, the apoptosis induced by *DIO-1* was completely blocked because of caspase inhibition, an observation that again clearly suggests that the death pathway induced by this gene requires caspase activity. Finally, extensive efforts to derive stable *DIO-1* transfectants in these three cell lines were unsuccessful, suggesting the lethality of *DIO-1* expression in these cells. All together, these results show that *DIO-1* overexpression results in the activation of a cell death program analogous to that operative in other systems, and that activation of the death pathway requires *DIO-1* translocation to the nucleus, where it probably performs a function compatible with its structure as a transcription factor.

Alteration of Limb Development by *DIO-1* Overexpression. Using whole-mount *in situ* hybridization, we also studied *DIO-1* expression throughout mouse development, which is expressed in the most distal limb cells on developmental day 10.5 (Fig. 4) and close to or within the limb interdigitating webs on day 12.5 (Fig. 4 Inset). Based on the *in vitro* effects and *in vivo* expression pattern described above, as well as on the presence of *DIO-1* transcripts in the limb cells undergoing

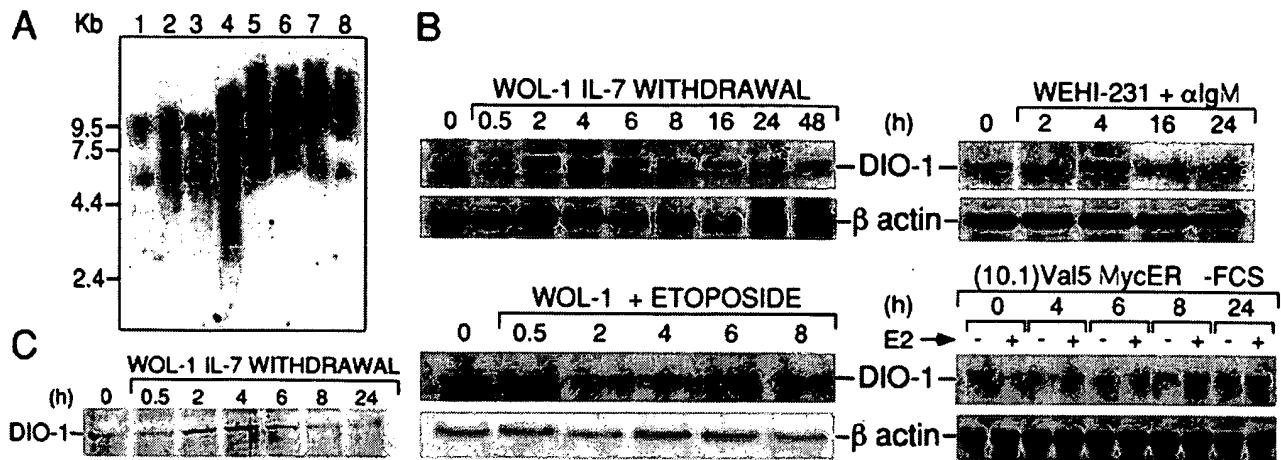


FIG. 2. *DIO-1* is differentially expressed under several apoptotic conditions and induces apoptosis when overexpressed. (A) *DIO-1* expression was analyzed in murine tissues by hybridization with the *DIO-1* riboprobe of a mouse MTN blot (CLONTECH). Molecular size markers are indicated on the left. Lanes: 1, heart; 2, brain; 3, spleen; 4, lung; 5, liver; 6, skeletal muscle; 7, kidney; 8, testis. (B) Northern blots containing 10 μ g per lane of total cytoplasmic RNA from the indicated cell lines, treated with several apoptotic stimuli at different time points, were hybridized to the *DIO-1* riboprobe. The blots were reprobated with an actin probe for normalization of the amounts loaded. (C) Western blot analysis of WOL-1 cells driven to apoptosis by IL-7 starvation. The position of the *DIO-1* gene product is indicated.

apoptotic cell death, we hypothesized that *DIO-1* may influence the control of cell proliferation and death during vertebrate limb development (see ref. 33 for a review on vertebrate limb outgrowth).

Retroviral technology was used to misexpress *DIO-1* in the chicken limb. A replication-competent retroviral vector containing the *DIO-1* ORF was injected into limb primordia at stages 10–23. The consequences of *DIO-1* expression were analyzed in embryo limb buds throughout development. At 60–72 h after injection, infected limb buds failed to develop a

normal apical ectodermal ridge (AER, the pseudo-stratified epithelium located at the tip of the limb, required for normal limb bud outgrowth) (Fig. 5 A and B). Maximal interference with limb outgrowth was observed when embryos were injected at stages 13–17. In 35% of the experiments performed at this stage, truncation occurred in the most distal elements, showing absence of digits, carpals, and metacarpals (Fig. 5 C and D). In the majority of cases (65%), however, reduction in size and malformation of the tibia and fibula are observed (Fig. 5 E and F). Misexpression before stage 13 caused alteration, but not truncation, in 12% of the cases; misexpression of *DIO-1* after stage 18 reduced malformation frequency to 40%, and no truncations were observed. These data indicate that to affect the phenotype of the developing limb bud, *DIO-1* must be expressed in a permissive environment and is not the consequence of nonspecific toxic effects. Finally, we analyzed the caspase activity level in the developing limbs. The maximal effects of *DIO-1* appear to correlate with maximum caspase activity (not shown), reinforcing the view that execution of the death program by *DIO-1* is caspase dependent, although *DIO-1* overexpression precedes caspase activity.

Because misexpression of *DIO-1* can perturb AER formation, we would expect this process to be preceded by changes in gene expression, in both the ectoderm and the underlying limb bud mesoderm. *In situ* hybridization of embryos infected with the *RCAS-DIO-1* construct by using riboprobes for me-

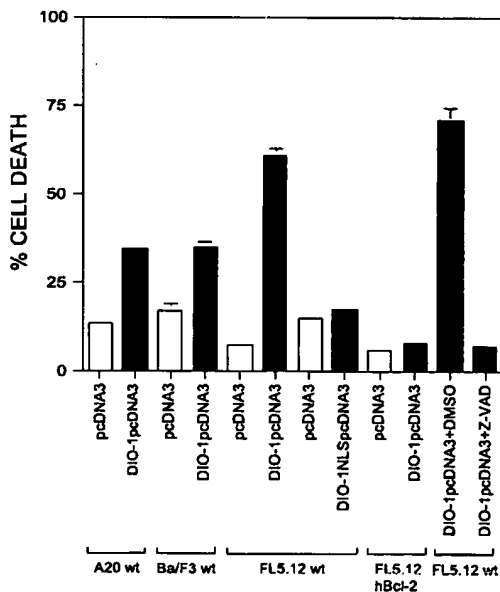


FIG. 3. *DIO-1* induces apoptosis *in vitro*. The *DIO-1* ORF was cloned into the pcDNA3 mammalian expression vector (Invitrogen). Both empty vector and the *DIO-1* construct were transiently transfected by electroporation into A20 and Ba/F3 cell lines. After 48-hr expression, the cells were permeabilized and stained with propidium iodide and cell cycle analyzed by FACS. FL5.12 wild-type and stably transfected hBcl-2 cells were transiently transfected as before. *DIO-1* (NLSpcDNA3 encodes a mutant protein lacking amino acids 162–192, which is therefore unable to translocate to the nucleus. Where indicated, the general caspase inhibitor Z-VAD-fmk (50 μ M final concentration; Bachem) was added immediately after transfection.

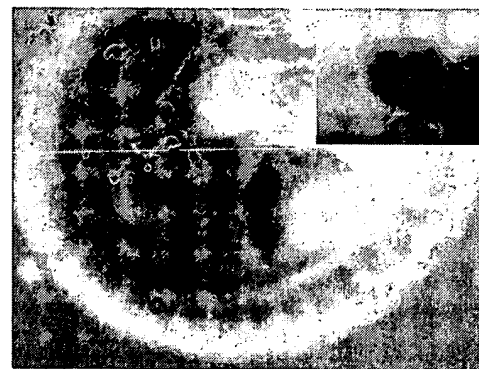


FIG. 4. Whole-mount *in situ* hybridization showing *DIO-1* expression pattern during murine development. Staining is shown of a 10.5-day mouse embryo and a 12.5-day mouse embryo limb (inset).

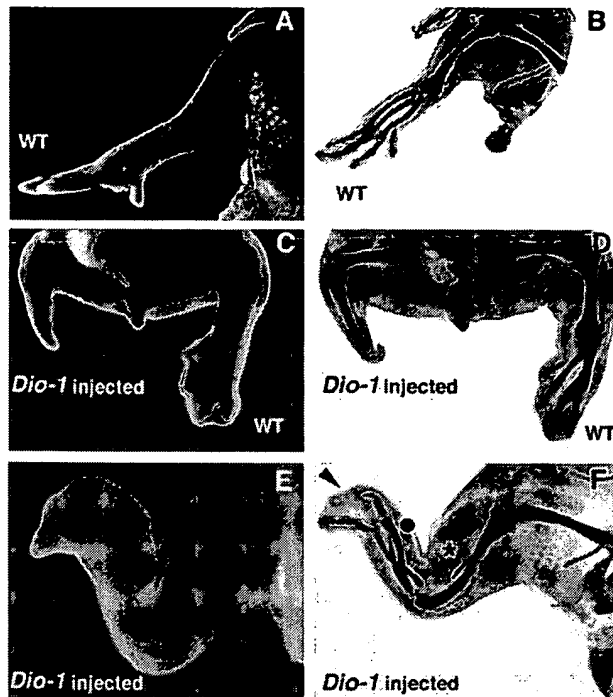


FIG. 5. *DIO-1* overexpression inhibits chicken limb outgrowth. A retroviral vector containing the *RCAS-DIO-1* construct was injected into limb primordia of stage 8–12 chicken embryos. Embryos were examined at different stages after infection. (A) Whole-mount preparation showing the hind limb of a wild-type embryo. (B) Alcian green staining of the same limb to visualize the normal cartilage pattern. (C) An infected embryo 6 days after injection, showing extensive truncation of the distal elements of the leg. (D) The same embryo after cartilage staining. Note the complete absence of elements distal to the tibia–fibula joint. (E and F) Whole-mount and cartilage staining of an embryo 8 days after infection with the *RCAS-DIO-1* construct. The infected limb is distorted and reduced in size, exhibiting an absence, reduction or malformation of phalanges, tarsals, and metatarsals (dot). In a few cases, the fibula was reduced in size (asterisk).

sodermal genes involved in limb outgrowth, such as *Msx-1* (Fig. 6A), *Lhx-2* (Fig. 6C), and *NF- κ B* (Fig. 6D), showed down-

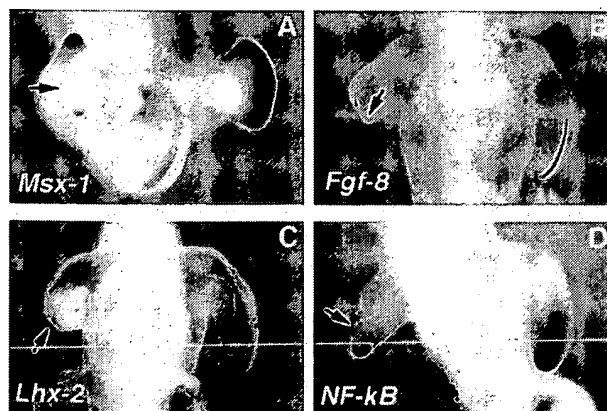


FIG. 6. *DIO-1* overexpression alters gene expression in the developing chicken limb bud. Misexpression of the *RCAS-DIO-1* construct leads to arrested limb outgrowth, preceded by changes in the expression of genes involved in outgrowth of the limb. Note the reduced size of the infected limb buds (left limb buds in all cases). Transcripts for *Msx-1* (A) *Fgf-8*; (B) *Lhx-2*; (C) and *NF- κ B* (D) are strongly down-regulated (arrows) in the injected limb buds (compare with the normal expression pattern in the uninjected limb bud, right limb bud in all cases).

regulation in their transcript levels. Transcripts for ectodermal genes involved in limb outgrowth, such as *Fgf-8*, are also absent or down-regulated (Fig. 6B). It is not known whether *DIO-1* misexpression is directly responsible for the down-regulation of ectodermal gene markers (i.e., *Fgf-8*), or if this is a consequence of the previously altered mesodermal gene expression. The combination of these results indicates that *DIO-1* may be important during limb development, and its apoptotic function may be a driving force in sculpting the final structure.

DISCUSSION

The apoptotic pathway is still elusive and, in many cases, depends on the outcome of the balance between levels of survival and apoptotic genes, at either the transcriptional or translational level. Here we report the cloning and characterization of a gene involved in apoptosis, which is up-regulated under certain apoptotic conditions that do not involve p53-mediated cell death. This up-regulation is observed quite early in cell death kinetics and always before any of the classical characteristics of apoptosis, i.e., DNA laddering, haploid subG₀/G₁ cell-cycle peak, or alteration of cell membrane polarity, can be detected. This indicates that *DIO-1* acts very early in the apoptotic cascade and suggests a key role in the control of the initiating triggering mechanism. This gene is a putative transcription factor, based on its sequence analysis, which may have a role in regulating the cell death process at the transcriptional level. Other genes with similar characteristics have been reported, including p53 (34), c-myc (16), or members of the glucocorticoid receptor family (35). Our studies demonstrate that *DIO-1* overexpression induces massive cell death, which can be blocked through overexpression of bcl-2, known to inhibit caspase activity (36–39). This indicates that *DIO-1* is upstream of the caspase cascade and that the induction of apoptosis driven by this gene proceeds through the main apoptotic route described so far. The Z-VAD-fmk blockade of *DIO-1*-induced apoptosis supports these conclusions.

The apoptotic mechanism activated by *DIO-1* requires its translocation to the nucleus; this finding, as well as its sequence and differential localization in living and apoptotic cells, can be used to draw inferences on its mode of function. *DIO-1* may thus be associated in the cytoplasm to a protein that prevents its entry into the nucleus, to which it must presumably be translocated to activate downstream mechanisms that initiate a caspase-executed apoptotic pathway. Such a mechanism is used by the nuclear transcription factor NF- κ B, which is maintained as a complex with I κ B in the cytoplasm until a given stimulus activates a caspase, leading to I κ B phosphorylation, ubiquitination, and degradation, releasing the NF- κ B proteins to traverse to the nucleus and activate gene transcription. A similar mechanism has been proposed for control of caspase-activated DNase and its translocation to the nucleus (7, 8).

To understand the *in vivo* role of this gene, we used the developing limb as a model. This system, which has been thoroughly characterized by developmental biologists, uses interference with limb outgrowth through modification of the gene expression pattern to analyze genes implicated in cell death. Here we have demonstrated that *DIO-1* affects chicken limb formation by general disruption of growth.

Limb buds infected with *DIO-1* constructs were reduced in size and failed to develop a defined AER. Severely truncated limbs with deformed and/or absent zeugopodal elements (most commonly the radius) and missing digits were also observed. After budding, continued limb outgrowth depends on correct AER formation. The reduced limb buds observed after *DIO-1* expression closely resemble the limb buds obtained after AER removal. All together, our experiments suggest that *DIO-1* overexpression perturbs maintenance of

AER function and hence limb outgrowth. Interestingly, the phenotypic changes caused by *DIO-1* misexpression kinetics, which result in altered limb development, appear to require the presence of the caspase activity required for elimination of interdigitating webs. *Fgf-8*, an AER-restricted gene involved in initiation and maintenance of limb outgrowth, is down-regulated or absent in infected limb buds, as are transcripts for *Msx-1* and *Lhx-2* genes involved in limb outgrowth whose expression is regulated by NF- κ B. It thus appears that allowing *DIO-1* protein translocation to the nucleus, down-regulation is observed for both mesodermal- and ectodermal-specific gene expression. It is unclear, however, whether this down-regulation occurs primarily in the mesoderm and indirectly in the AER or, alternatively, whether down-regulation of gene expression occurs initially in the AER and subsequently in the mesoderm. Identification of the mechanisms of action of *DIO-1* may be instrumental in answering this question and may provide another missing link in the identification of the mechanism that controls cell proliferation and cell death. In contrast to the consequences of *DIO-1* overexpression, ectopic NF- κ B expression does not lead to significant morphological perturbations (data not shown). In sum, it appears that some proteins, such as NF- κ B, control the cell proliferation and outgrowth of the vertebrate limb, whereas others, such as *DIO-1*, promote cell death. The integral process of limb outgrowth would thus require a balanced interaction between both forces.

We thank Drs. R. S. Geha, M. Izquierdo, D. Green, and J. Hurlé for reading the manuscript and C. Mark for editorial assistance. This work was funded in part by a grant from the Dirección General de Educación Superior e Investigación (DGESI) (Spain). D.G.-D. is the recipient of a fellowship from the Spanish Ministerio de Educación y Ciencia. The Department of Immunology and Oncology, Centro Nacional de Biotecnología, Universidad Autónoma, Madrid, was founded and is supported by the Spanish Research Council (CSIC) and Pharmacia & Upjohn.

- Jacobson, M. D., Weil, M. & Raff, M. C. (1997) *Cell* **88**, 347–354.
- Raff, M. C., Barres, B. A., Burne, J. F., Coles, H. S., Ishizaki, Y. & Jacobson, M. D. (1993) *Science* **262**, 695–700.
- Vucic, D., Kaiser, W. J., Harvey, A. J. & Miller, L. K. (1997) *Proc. Natl. Acad. Sci. USA* **94**, 10183–10188.
- Irmeler, M., Thome, M., Hahne, M., Scheider, P., Hofmann, K., Steiner, V., Bodmer, J.-L., Schröter, M., Burns, K., Mattmann, C., *et al.* (1997) *Nature (London)* **388**, 190–195.
- Ghayur, T., Banerjee, S., Hugunin, M., Butler, D., Herzog, L., Carter, A., Quintal, L., Sekut, L., Talanian, R., Paskind, M., *et al.* (1997) *Nature (London)* **386**, 619–623.
- Izquierdo, M., Grandien, A., Criado, L. M., Robles, S., Leonardo, E., Albar, J. P., González de Buitrago, G. & Martínez-A, C. (1999) *EMBO J.* **18**, 156–166.
- Enari, M., Sakahira, H., Yokoyama, H., Okawa, K., Iwamatsu, A. & Nagata, S. A. (1998) *Nature (London)* **391**, 43–50.
- Sakahira, H., Enari, M. & Nagata, S. (1998) *Nature (London)* **391**, 96–99.
- Clavería, C., Albar, J. P., Buesa, J. M., Barbero, J. L., Martínez-A, C. & Torres, M. (1998) *EMBO J.* **17**, 7199–7208.
- Martin, D. P., Schmidt, R. E., DiStefano, P. S., Lowry, O. H., Carter, J. G. & Johnson, E. M., Jr. (1988) *J. Cell Biol.* **106**, 829–844.
- Schwartz, L. M., Kosz, L. & Kay, B. K. (1990) *Proc. Natl. Acad. Sci. USA* **87**, 6594–6598.
- Wagner, A. J., Kokontis, J. M. & Hay, N. (1994) *Genes Dev.* **8**, 2817–2830.
- Chong, L. E.-C., Chan, F. K.-M., Cado, D. & Winoto, A. (1997) *EMBO J.* **16**, 1865–1875.
- Cohen, J. J. & Duke, R. C. (1984) *J. Immunol.* **132**, 38–42.
- Kumar, A., Commene, M., Flickinger, T. W., Horvath, C. M. & Stark, G. R. (1997) *Science* **278**, 1630–1632.
- Evan, G. I., Wyllie, A. H., Gilbert, C. S., Littlewood, T. D., Land, H., Brooks, M., Waters, C. M., Penn, L. Z. & Hancock, D. C. (1992) *Cell* **69**, 119–128.
- Ham, J., Babij, C., Whitfield, J., Pfarr, C. M., Lallemand, D., Yaniv, M. & Rubin, L. L. (1995) *Neuron* **14**, 927–939.
- Baichwal, V. R. & Baeuerle, P. A. (1997) *Curr. Biol.* **7**, 94–96.
- White, K., Grether, M. E., Abrams, J. M., Young, L., Farrell, K. & Steller, H. (1994) *Science* **264**, 677–683.
- Grether, M. E., Abrams, J. M., Agapite, J., White, K. & Steller, H. (1995) *Genes Dev.* **9**, 1694–1708.
- Chen, P., Nordstrom, W., Gish, B. & Abrams, J. M. (1996) *Genes Dev.* **10**, 1773–1782.
- Kanegae, Y., Tavares, A. T., Izpisua Belmonte, J. C. & Verma, I. M. (1998) *Nature (London)* **392**, 611–614.
- Sambrook, J., Fritsch, E. F. & Maniatis, T. (1989) in *Molecular Cloning: A Laboratory Manual*, 2nd Ed. (Cold Spring Harbor Lab. Press, Plainview, NY).
- Wilkinson, D. G. (1993) in *In Situ Hybridisation*, ed. Wilkinson, D. G. (Oxford Univ. Press, Oxford).
- Izpisua Belmonte, J. C., De Robertis, E. M., Storey, K. G. & Stern, C. (1993) *Cell* **74**, 645–659.
- Robert, B., Lyons, G., Simandl, B.-K., Kuroiwa, A. & Buckingham, M. (1991) *Genes Dev.* **5**, 2363–2374.
- Vogel, A., Rodriguez, C. & Izpisua Belmonte, J. C. (1996) *Development (Cambridge, U.K.)* **122**, 1737–1750.
- Morgan, B. A., Izpisua Belmonte, J. C., Duboule, D. & Tabin, C. J. (1992) *Nature (London)* **358**, 236–239.
- Liang, P. & Pardee, A. B. (1992) *Science* **257**, 967–971.
- Altschul, S. F., Gish, W., Miller, W., Myers, E. W. & Lipman, D. J. (1990) *J. Mol. Biol.* **215**, 403–410.
- Kozak, M. (1987) *Nucleic Acids Res.* **15**, 8125–8148.
- Brás, A., Ruiz-Vela, A., González de Buitrago, G. & Martínez-A, C. (1999) *FASEB J.* **13**, 931–944.
- Schwabe, J., Rodriguez-Esteban, C. & Izpisua Belmonte, J. C. (1998) *Trends Genet.* **14**, 229–235.
- Polyak, K., Xia, Y., Zweir, J. L., Kinzler, K. W. & Vogelstein, B. (1997) *Nature (London)* **389**, 300–305.
- Lososa, E., King, L. B. & Ashwell, J. D. (1998) *Immunity* **8**, 67–76.
- Kluck, R. M., Bossy-Wetzel, E., Green, D. R. & Newmeyer, D. D. (1997) *Science* **275**, 1132–1136.
- Adams, J. M. & Cory, S. (1998) *Science* **281**, 1322–1325.
- Huang, D., Adams, J. M. & Cory, S. (1998) *EMBO J.* **17**, 1029–1039.
- Cuende, E., Ales-Martínez, J. E., Ding, L., González, M., Martínez-A, C. & Núñez, G. (1993) *EMBO J.* **12**, 1555–1560.

Death Inducer-Obliterator 1 Triggers Apoptosis after Nuclear Translocation and Caspase Upregulation

David García-Domingo, Dorian Ramírez,[†] Gonzalo González de Buitrago, and Carlos Martínez-A*

Department of Immunology and Oncology, Centro Nacional de Biotecnología/CSIC, Universidad Autónoma de Madrid, Campus de Cantoblanco, E-28049 Madrid, Spain

Received 22 July 2002/Returned for modification 4 September 2002/Accepted 4 February 2003

Death inducer-obliterator 1 (DIO-1) is a gene that is upregulated early in apoptosis. Here we report that in healthy cells, the DIO-1 gene product was located in the cytoplasm, where it formed oligomers. After interleukin-3 starvation or c-Myc-induced apoptosis in serum-free conditions, DIO-1 translocated to the nucleus, where it upregulated caspase levels and activity. A nuclear localization signal deletion mutant (DIO-1ΔNLS) was unable to translocate to the nuclear compartment in the absence of interleukin-3 and failed to upregulate procaspase levels or trigger cell death. In addition, cells stably expressing DIO-1ΔNLS were protected from apoptosis induced by interleukin-3 withdrawal. These results indicate that DIO-1 has a relevant role in regulating the early stages of cell death.

Apoptosis, or programmed cell death, has a major role in normal development, tissue homeostasis, defense against viral invasion, immune modulation, and, when dysregulated, modulation of autoimmune and clonal or neoplastic diseases (15, 17, 30). Apoptosis is characterized by cell shrinkage, chromatin condensation, internucleosomal DNA cleavage, membrane blebbing, and the formation of apoptotic bodies that are phagocytosed by other cells (8, 38). These morphological changes are orchestrated by the activity of a family of aspartate-specific proteases called caspases (4, 7, 34).

Caspases are produced in cells as catalytically inactive zymogens, or procaspases, composed of three subunits, a prodomain and two catalytic subdomains, known as the large and small subunits (1). Procaspases must be proteolytically processed to become active proteases. An effector caspase, for example caspase 3, is activated by an initiator caspase, such as caspase 9, through proteolytic cleavage at specific internal Asp residues to give rise to the two subunits of the mature caspase. Once activated, the effector caspases cleave a broad spectrum of cellular targets, leading ultimately to cell death (38). Activation of the initiator caspases is in turn regulated by upstream protein complexes. In the case of the so-called “extrinsic” pathway, activation of death receptors such as Fas/CD95 and tumor necrosis factor receptor 1 after binding of their respective ligands induces recruitment of caspase 8 (FLICE) via the adapter molecule FADD (Fas-associated protein with death domain) (27). Caspase 8 can activate effector caspases either directly (3, 27) or indirectly by cleaving Bid and inducing the release of mitochondrial cytochrome *c* (18, 25).

In the case of the “intrinsic” death receptor-independent pathway, apoptotic cell death is induced directly by death stimuli and is also regulated by adapter complexes. This is the case

of one of the major routes to caspase activation pathways, triggered by cytochrome *c* release from the mitochondrial intermembrane space into the cytosol (23). Cytosolic cytochrome *c* promotes assembly of a protein complex called the apoptosome, which includes caspase 9 bound to the CED-4 homolog Apaf-1 (19, 42), inducing autoactivation of procaspase 9 (33, 37). Following activation, caspase 9 cleaves and activates procaspase 3 (19, 42), giving rise to a proteolytic cascade involving multiple caspases.

DIO-1 was identified by a differential display approach (21) in WOL-1 pre-B cells induced to undergo apoptosis by interleukin-7 (IL-7) starvation (9). Its predicted amino acid sequence showed transcriptional activation domains, a canonical bipartite nuclear localization signal (NLS), a PhD finger, and a carboxy-terminal lysine-rich region. DIO-1 mRNA was upregulated soon after apoptotic induction by several stimuli, including removal of IL-7, addition of dexamethasone or gamma interferon in WOL-1 cells, immunoglobulin M (IgM) receptor cross-linking in WEHI-231 cells, or *c-myc* activation under serum-free conditions in the absence of p53 expression in MEF(10.1)Val5MycER cells. Overexpression of DIO-1 in cells or misexpression in chick limbs induced massive apoptosis in the absence of any apoptotic stimuli; this could be inhibited by Bcl-2 overexpression or incubation with the general caspase inhibitor benzoyloxycarbonyl-Val-Ala-Asp-fluoromethyl ketone (z-VAD-fmk). These results suggested that DIO-1-induced apoptosis requires caspase activation. Furthermore, overexpression of a DIO-1 deletion mutant lacking both NLSs failed to induce cell death, linking its lack of lethality to an inability to translocate.

Here we studied the mechanism by which DIO-1 induces apoptosis and the importance of its subcellular localization. We generated several tagged constructs and analyzed the subcellular distribution pattern of both wild-type and mutant DIO-1 in various apoptotic situations, revealing nuclear translocation as the main regulatory event in the DIO-1-activated apoptotic pathway. We provide evidence that DIO-1 translocation boosts the apoptotic machinery by upregulating protein

* Corresponding author. Mailing address: Department of Immunology and Oncology, Centro Nacional de Biotecnología/CSIC, UAM Campus de Cantoblanco, E-28049 Madrid, Spain. Phone: 34 91 585 45 59. Fax: 34 91 372 04 93. E-mail: cmartinez@cnb.uam.es.

[†] Present address: University of Michigan Medical School, Ann Arbor, MI 48109.

levels of procaspase 3 and 9, which enhances their apoptosis-inducing activity.

MATERIALS AND METHODS

Expression plasmids. DIO-1ΔNLSpcDNA3 was generated from DIO-1 (cloned in pcDNA3 by reverse PCR with the circular plasmid as the template and the primers 5'-GAAGATTCTGCCGAACTGGG-3' and 5'-AAGTTCCTTC AACGTAAGG-3', which span the NLSs and the connecting sequence; the PCR product was permitted to further self-ligate. Both N-terminally Flag-tagged DIO-1 and DIO-1ΔNLS were PCR amplified from their corresponding pcDNA3 constructs with a proof-reading polymerase and the primers 5'-GCGGATCCG ATGATAAAGGGCACCTG-3' and 5'-CGACCTCGAGTTACCAAGGCCTA AACTG-3' for in-frame reading. The PCR products were digested with *Bam*HI and *Xho*I and subcloned into the pCMV-Tag 2B vector (Stratagene). DIO-1/Myc was generated similarly after PCR amplification with the primers 5'-TGGAATTCACCATGGATGATAAAGGGCAC-3' and 5'-GCTCTAGA CCAAGGCCTAAACTG-3' from DIO-1pcDNA3, digested with *Eco*RI and *Xba*I, and subcloned into the pEF4/Myc-His A vector (Invitrogen). All constructs were verified by nucleotide sequencing.

Cell culture. FL5.12 and MEF(10.1)Val5MycER cells were cultured as described previously (9). 293T cells were cultured in Dulbecco's modified Eagle's medium supplemented with 10% fetal bovine serum, 2 mM L-glutamine, and antibiotics.

Antibodies and reagents. Production of the polyclonal antibody against murine DIO-1 amino acids 58 to 72 has been described (9). Polyclonal rabbit anti-mouse caspase 3 was the kind gift of T. Mak and R. Hakem (Ontario Cancer Institute, Toronto, Canada); anti-caspase 9 was the kind gift of D. R. Green and B. Wolf (39). Anti-Flag M2 monoclonal antibody (Sigma), anti-Myc 9E10 monoclonal antibody (Santa Cruz Biotechnologies), protein A-agarose (Sigma), protein G-agarose (Sigma), antiphosphoserine sampler kit (Biomol), antiphosphoserine monoclonal antibody (Calbiochem), and antiphosphothreonine monoclonal antibody (Calbiochem) were purchased as indicated. z-VAD-fmk was purchased from Bachem.

Establishment of FL5.12 cells stably overexpressing DIO-1ΔNLS. FL5.12 cells (3×10^6) were electroporated with 10 μg of DIO-1ΔNLS construct or pcDNA3. Transfected cells were resuspended in 48 ml of complete medium and distributed in a 48-well plate. Selection was performed after 24 h by removing the medium and adding fresh complete medium containing 1 mg of G418 per ml. Selection was carried out for 30 days, and DIO-1ΔNLS expression was determined by reverse transcription-PCR and Western blotting.

Subcellular fractionation. FL5.12 cells (2×10^7) were harvested and washed in ice-cold phosphate-buffered saline (PBS), and pellets were resuspended in 5 volumes of ice-cold buffer A (10 mM HEPES [pH 8.0], 0.5 M sucrose, 1 mM EDTA, 0.5 mM spermidine, 0.15 mM spermine, 15 mM KCl, 0.5 mM dithiothreitol, 10 μg of aprotinin per ml, 10 μg of pepstatin A per ml, 10 μg of leupeptin per ml, 1 mM phenylmethylsulfonyl fluoride [PMSF], 100 μM Na₃VO₄, and 10 mM NaF). After incubation on ice for 15 min, cells were lysed by three freeze-thaw cycles and centrifuged ($1,000 \times g$, 10 min, 4°C), and the nuclear pellet was resuspended in buffer B (10 mM piperazine-N,N'-bis(2-ethanesulfonic acid) [PIPES, pH 7.4], 80 mM KCl, 20 mM NaCl, 5 mM sodium EGTA, 250 mM sucrose, 1 mM dithiothreitol, 10 μg of aprotinin per ml, 10 μg of pepstatin A per ml, 10 μg of leupeptin per ml, 1 mM PMSF, 100 μM Na₃VO₄, and 10 mM NaF) at 8.5×10^7 nuclei/ml. Samples were separated by sodium dodecyl sulfate-polyacrylamide gel electrophoresis (SDS-PAGE) under reducing conditions. Purity of the cytosolic and nuclear fractions was tested by Western blotting with compartment-specific antibodies to procyclic acidic repetitive protein and calpain-1 (not shown).

Transfections and immunoprecipitation. Transient transfections in FL5.12 and MEF(10.1)Val5MycER cells were performed by electroporation as described previously (9). 293T cells were transiently transfected in six-well plates with Lipofectamine Plus (Life Technologies) following the manufacturer's protocol. Cytosolic extracts for immunoprecipitation were obtained after cell lysis in NP-40 buffer (40 mM Tris-HCl [pH 8], 500 mM NaCl, 0.1% NP-40, 6 mM EDTA, 6 mM EGTA, 10 μg of aprotinin per ml, 10 μg of pepstatin A per ml, 10 μg of leupeptin per ml, 1 mM PMSF, 100 μM Na₃VO₄, and 10 mM NaF) or a digitonin-containing buffer (10 mM triethanolamine [pH 8], 150 mM NaCl, 1 mM EDTA, 10% glycerol, 1% digitonin, 10 μg of aprotinin per ml, 10 μg of pepstatin A per ml, 10 μg of leupeptin per ml, 1 mM PMSF, 100 μM Na₃VO₄, and 10 mM NaF). Immunoprecipitation was performed by preclearing lysates with 30 μl of protein A/G-agarose (1 h, 4°C, with gentle rotation), followed by incubation with the appropriate antibody (10 μg/ml; 1 h, 4°C). After addition of protein A- or protein G-agarose (30 μl), beads were pelleted by brief centrifugation and washed three

times in 50 mM Tris-HCl (pH 7.6) buffer, and the pellet was boiled in loading buffer and analyzed in Western blot.

Phosphatase treatment. 293T cells transiently transfected with Flag-tagged DIO-1 were harvested, washed in ice-cold PBS, and lysed in a digitonin-containing buffer (40 mM Tris-HCl [pH 8], 50 mM NaCl, 2 mM MnCl₂, 1% digitonin, 10 μg of aprotinin per ml, 10 μg of pepstatin A per ml, 10 μg of leupeptin per ml, 1 mM PMSF). After removal of cellular debris by centrifugation, lysates were treated with 500 U of λ-phosphatase (Calbiochem) (30 min, 30°C). The reaction was terminated by addition of loading buffer and then analyzed in Western blot.

Western blot analysis. Cells for analysis of procaspase expression were washed with PBS, and the pellet was suspended in lysis buffer (137 mM NaCl, 20 mM Tris-HCl [pH 8], 1 mM MgCl₂, 1 mM CaCl₂, 10% glycerol, 1% NP-40, 0.5% deoxycholate, 0.1% SDS, 10 μg of aprotinin per ml, 10 μg of pepstatin A per ml, 10 μg of leupeptin per ml, and 1 mM PMSF) for 30 min on ice. The protein content of the lysates was quantified with the Bio-Rad DC protein assay (Bio-Rad); after SDS-PAGE, proteins were transferred to nitrocellulose membranes (Bio-Rad). Equal protein loading was verified by Ponceau Red (Sigma) staining. Membranes were blocked overnight with 5% nonfat dry milk in TBS buffer (20 mM Tris-HCl [pH 7.5], 150 mM NaCl); subsequent incubations and membrane washes were performed in TBS-T buffer (20 mM Tris-HCl [pH 7.5], 150 mM NaCl, and 0.2% Tween 20) containing 1% nonfat dry milk. After 2 h of antibody incubation and 1 h of washing, blots were developed with peroxidase-conjugated anti-rabbit or anti-mouse immunoglobulin antibodies (Dako), and proteins were detected by an enhanced chemiluminescence system (ECL; Amersham).

Fluorescence microscopy. For immunofluorescence, cells were cultured on coverslips, washed in PBS, fixed in 4% paraformaldehyde (15 min, room temperature), washed three times in PBT (PBS with 0.1% Tween 20), incubated in 2% bovine serum albumin, and incubated for 1 h with anti-DIO-1 (1:100) or anti-Flag M2 (1:500) in PBT. After incubation, cells were washed three times in the same buffer and incubated for 1 h with indocarbocyanine-conjugated secondary antibodies (Jackson ImmunoResearch). After washing, samples were incubated with Sybr Green (Molecular Probes) in PBS for DNA staining. Serial Z-sections were obtained with an Ar-Kr laser and a TCS-NT Leica confocal imaging system.

Enzyme assay for caspase activity. Cells were collected, washed with ice-cold PBS, and resuspended in extraction buffer (50 mM Tris-HCl [pH 7.6], 150 mM NaCl, 0.5 mM EDTA, 10 mM NaH₂PO₄, 10 mM Na₂HPO₄, 1% Nonidet P-40, 0.4 mM Na₃VO₄, 1 mM PMSF, 10 μg of aprotinin per ml, 10 μg of pepstatin A per ml, 10 μg of leupeptin per ml). After incubation (30 min, on ice), the cell lysate was centrifuged ($20,000 \times g$, 30 min), and the supernatant was used as the cytosolic extract. Five micrograms of cytosolic proteins, estimated by the bicinchoninic acid method (36), were diluted fivefold in assay buffer (25 mM HEPES [pH 7.5], 0.1% CHAPS, 10% sucrose, 10 mM dithiothreitol, and 0.1 mg of ovalbumin per ml) and incubated (1 h, 37°C) with 10 μM of the fluorescent substrate Ac-DEHD-AMC (acetyl-Asp-Glu-His-Asp-7-amino-4-methylcoumarin), Ac-DEVD-AMC (acetyl-Asp-Glu-Val-Asp-7-amino-4-methylcoumarin), Ac-VEID-AMC (acetyl-Val-Glu-Ile-Asp-7-amino-4-methylcoumarin), or Ac-LEHD-AMC (acetyl-Leu-Glu-His-Asp-7-amino-4-methylcoumarin) to measure caspase 2, caspase 3-like, caspase 6, and caspase 9 activity, respectively. The reaction was terminated by addition of high-pressure liquid chromatography (HPLC) buffer (water-acetonitrile [75:25], 0.1% trifluoroacetic acid). Cleaved substrate fluorescence was determined by C₁₈ reverse-phase HPLC with fluorescence detection (338 nm excitation, 455 nm emission). Control experiments confirmed linearity with time and protein concentration of substrate release.

Apoptosis assay. Apoptosis was evaluated by staining cellular DNA content with the DNA intercalator propidium iodide in a semiautomatic procedure (DNA-Prep Reagents; Coulter), followed by analysis on an Epics XL flow cytometer (Coulter). Briefly, cells (10^5 to 10^6) were recovered by centrifugation, resuspended in 100 μl of PBS, permeabilized, and stained by adding 100 μl of detergent reagent followed by 1 ml of propidium iodide solution. After mixing, samples were incubated (37°C, 1 h) and analyzed by flow cytometry.

RESULTS

DIO-1 nuclear translocation following apoptotic stimulation requires the NLS

We previously reported differences in DIO-1 mRNA levels after induction of p53-dependent and -independent apoptosis in MEF(10.1)Val5MycER cells (9). DIO-1 transcripts were upregulated in apoptotic processes in a p53-independent fashion. The presence of two putative NLSs in the DIO-1 gene product suggested that it may be localized

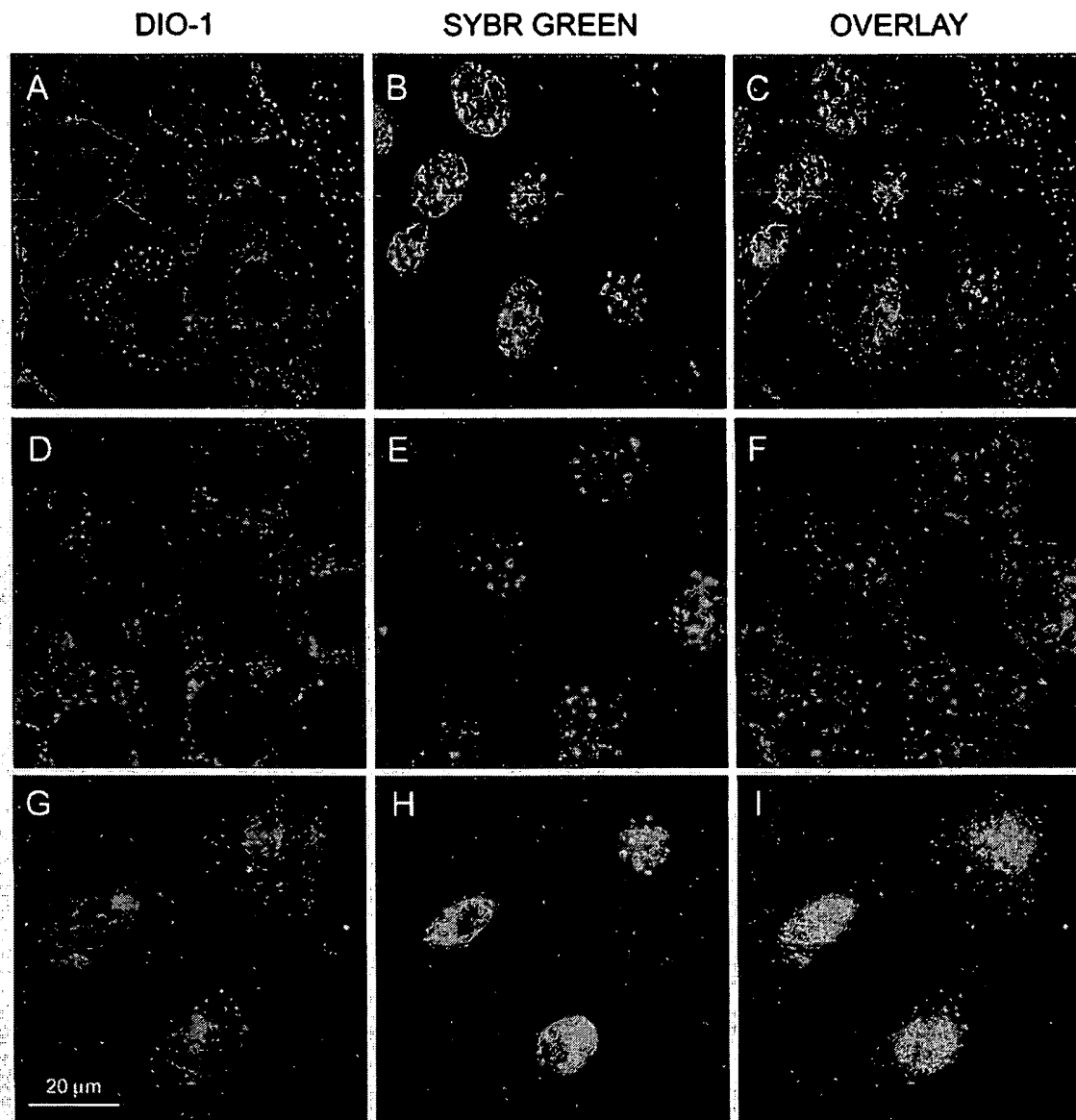


FIG. 1. Immunolocalization of endogenous DIO-1 under apoptotic conditions. (A to C) Viable (nonapoptotic) MEF(10.1)Val5MycER cells were stained with anti-DIO-1 antibody (red); nuclei were stained with Sybr Green (green). (D to F) The same cells were induced to apoptosis by lowering the incubation temperature (32°C, 12 h) to activate p53 in the presence of 17 β -estradiol (1 μ M). Note the clear cytoplasmic pattern of DIO-1, although some cells have already begun the apoptotic program. (G to I) The same cell line, incubated at 39°C to inactivate p53, was 17 β -estradiol treated (1 μ M) and serum starved for 8 h, the time at which DIO-1 mRNA is upregulated. Note nuclear translocation of DIO-1 to the intact, nonapoptotic nuclei.

in the nucleus (9). To study its putative role as a transcription factor, we examined the subcellular localization pattern of the DIO-1 gene product and its NLS deletion mutant (DIO-1 Δ NLS). Immunofluorescence microscopy of healthy MEF(10.1)Val5MycER cells with an affinity-purified rabbit antiserum specific for a DIO-1 peptide (9) indicated a clear cytoplasmic pattern for the DIO-1 protein, which was nearly absent in the nucleus (Fig. 1A to C). p53-mediated triggering of apoptosis showed no change in the DIO-1 localization pattern (Fig. 1D to F), although the cells underwent apoptosis (not shown). Cells cultured at 39°C to inactivate p53, then

induced to apoptosis by 17 β -estradiol addition and fetal bovine serum starvation, showed DIO-1 translocation from cytoplasm to the nucleus (Fig. 1G to I). This was observed before cell death was detectable by any method and in parallel to mRNA upregulation kinetics.

We examined the subcellular localization of the DIO-1 Δ NLS mutant, but as the anti-DIO-1 antibody recognizes both wild-type and mutant proteins, the mutant was Flag tagged (DIO-1 Δ NLS/Flag) and transiently transfected into MEF(10.1)Val5MycER cells. Apoptosis was induced 24 h post-transfection, and staining was performed at the same time

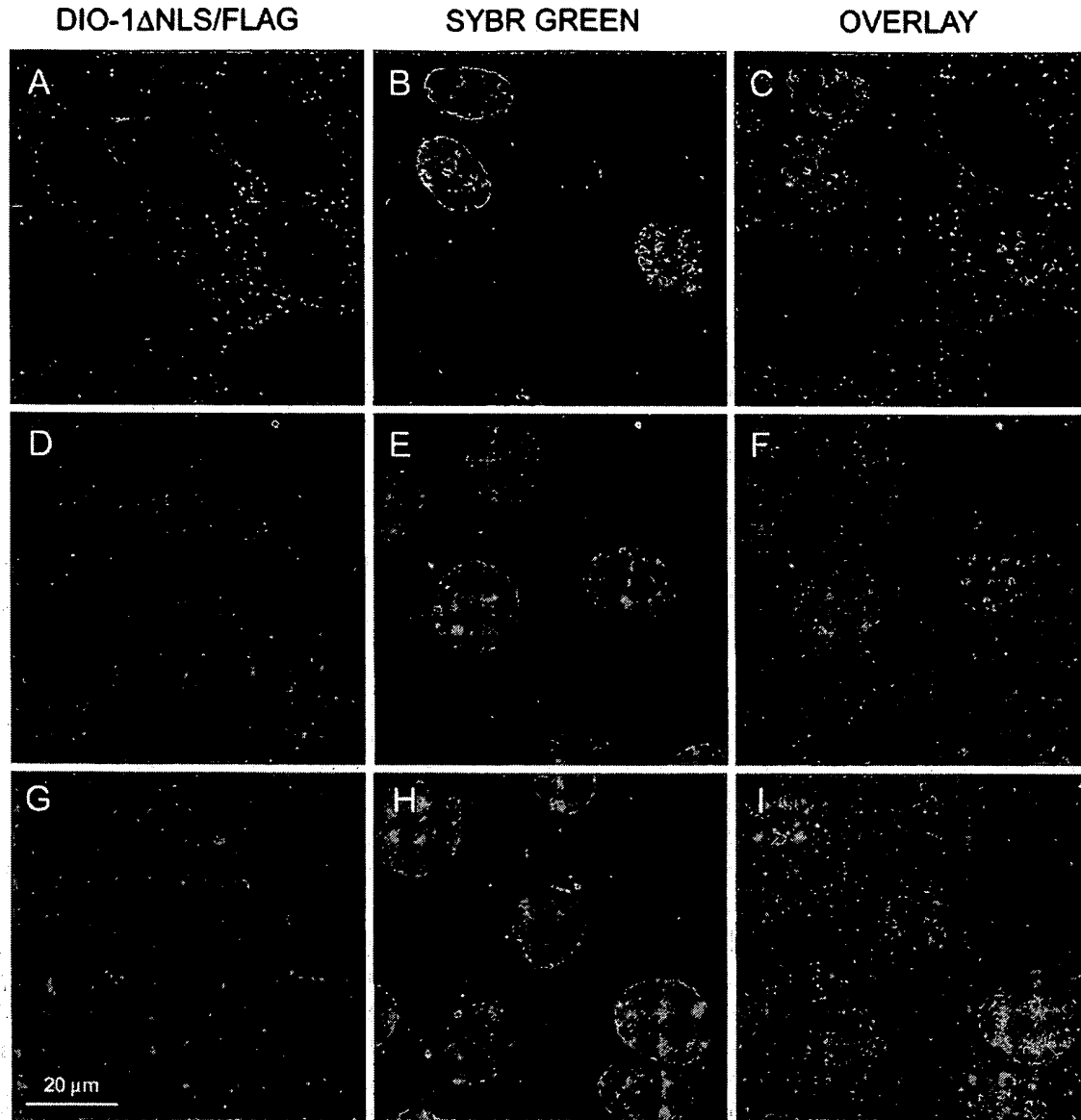


FIG. 2. Immunolocalization of DIO-1 Δ NLS in MEF(10.1)Val5MycER cells under apoptotic conditions. A DIO-1 Δ NLS Flag-tagged construct was transiently transfected into the cells, which were analyzed 36 h posttransfection. A selected field of positive cells is shown. (A to C) Viable cells were stained with anti-Flag antibody (red) and Sybr Green (green). (D to F) Conditions as for Fig. 1D to F. (G to I) Conditions as for Fig. 1G to I. The protein did not translocate to the nucleus in the presence of the stimulus that induced wild-type DIO-1 translocation.

points as for wild-type DIO-1. A clear cytoplasmic pattern was observed in healthy cells (Fig. 2A to C) and in those undergoing p53-induced apoptosis (Fig. 2D to F). DIO-1 Δ NLS was unable to translocate to the nucleus under conditions that promoted translocation of the wild-type form (Fig. 2G to I), as predicted by its lack of NLS.

DIO-1 forms oligomers. To test for the association state of DIO-1, we fused murine DIO-1 to N-terminal Flag (DIO-1/Flag) and C-terminal Myc (DIO-1/Myc) tags in different constructs. The constructs were coexpressed by transient transfection into human embryonic kidney 293T cells, and proteins were isolated under nondenaturing conditions with buffers that permitted cytosolic extraction. Western blot analysis with the

anti-DIO-1 antibody (Fig. 3A) and antitag antibodies (Fig. 3B) confirmed expression in total lysates of cells transfected with the appropriate plasmids, but not in cells transfected with control plasmids. In all cases, a triplet was observed with very close bands. The triplets do not correspond to proteolytic degradation products, as they were detected equally well with antibodies to tags located at both ends of the protein, in the presence of large amounts of protease inhibitors. These multiple bands are more likely to represent posttranslational modifications of DIO-1.

Oligomerization was determined in an immunoprecipitation assay performed with anti-Myc and resolved in SDS-polyacrylamide gel electrophoresis (SDS-PAGE). Subsequent Western

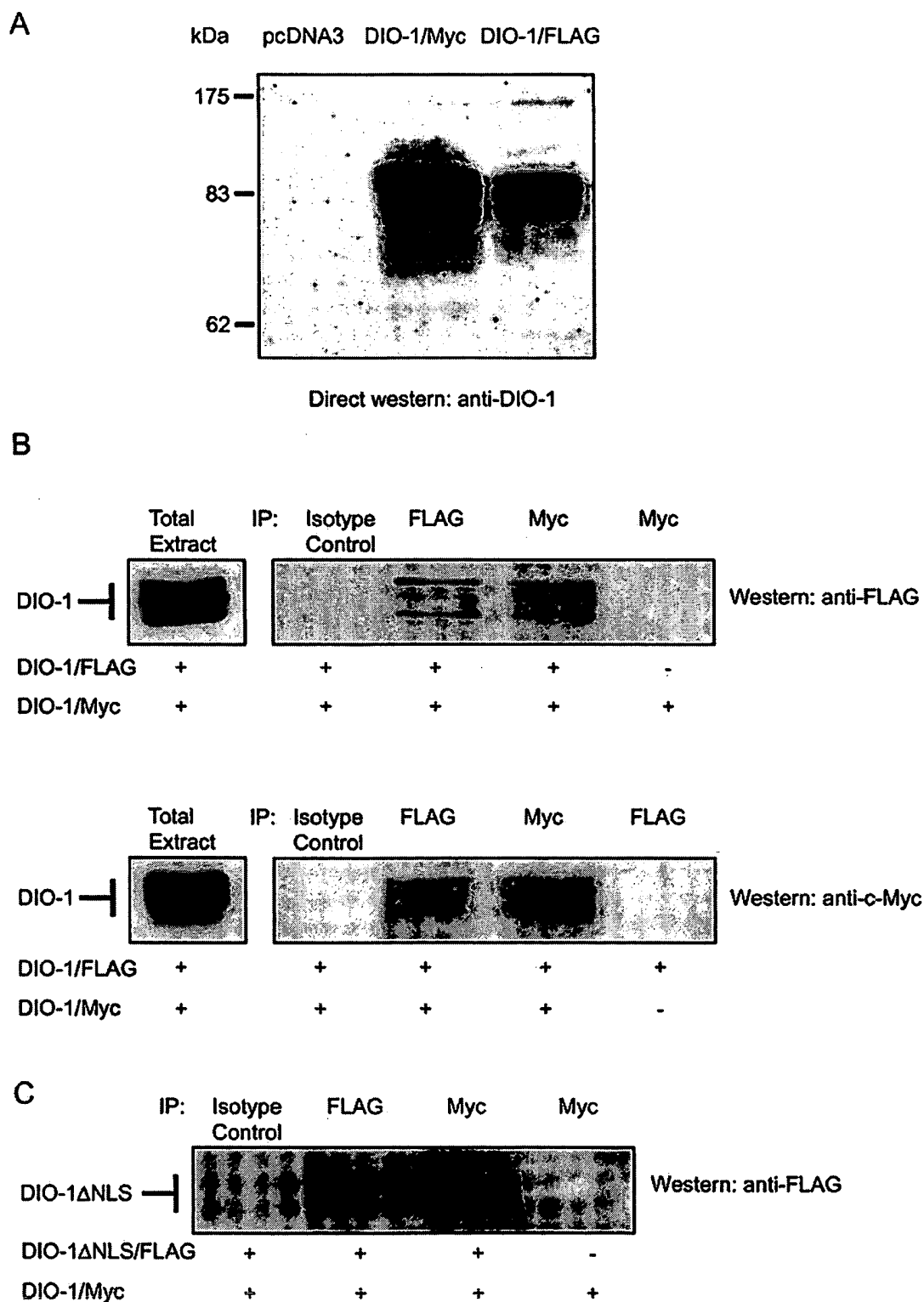


FIG. 3. DIO-1 forms oligomers. (A) Expression of DIO-1 gives rise to a three-band pattern in Western blot. Whole-cell extracts from 293T cells transfected with vector plasmid (pcDNA3) or expression plasmids encoding Myc- or Flag-tagged DIO-1 were analyzed in Western blot with the anti-DIO-1 antibody. Molecular size markers are indicated at the left. (B) 293T cells were cotransfected with constructs encoding Myc- and Flag-tagged DIO-1 except for the last lane, in which only one construct was transfected as a negative immunoprecipitation control. After 48 h, extracts were immunoprecipitated with anti-Flag or anti-Myc monoclonal antibody. An irrelevant isotype-matched antibody was used as a control. Immunoprecipitates were analyzed by SDS-PAGE and blotted with anti-Flag (upper panel) or anti-Myc antibody (lower panel). Total cell extracts were also analyzed by SDS-PAGE and blotted with the same antibodies (left). (C) 293T cells were cotransfected with constructs encoding Myc-tagged DIO-1 and Flag-tagged DIO-1ΔNLS except for the last lane, in which only DIO-1/Myc was transfected. The experimental procedure was identical to that for panel B, upper panel. All results are representative of three independent experiments.

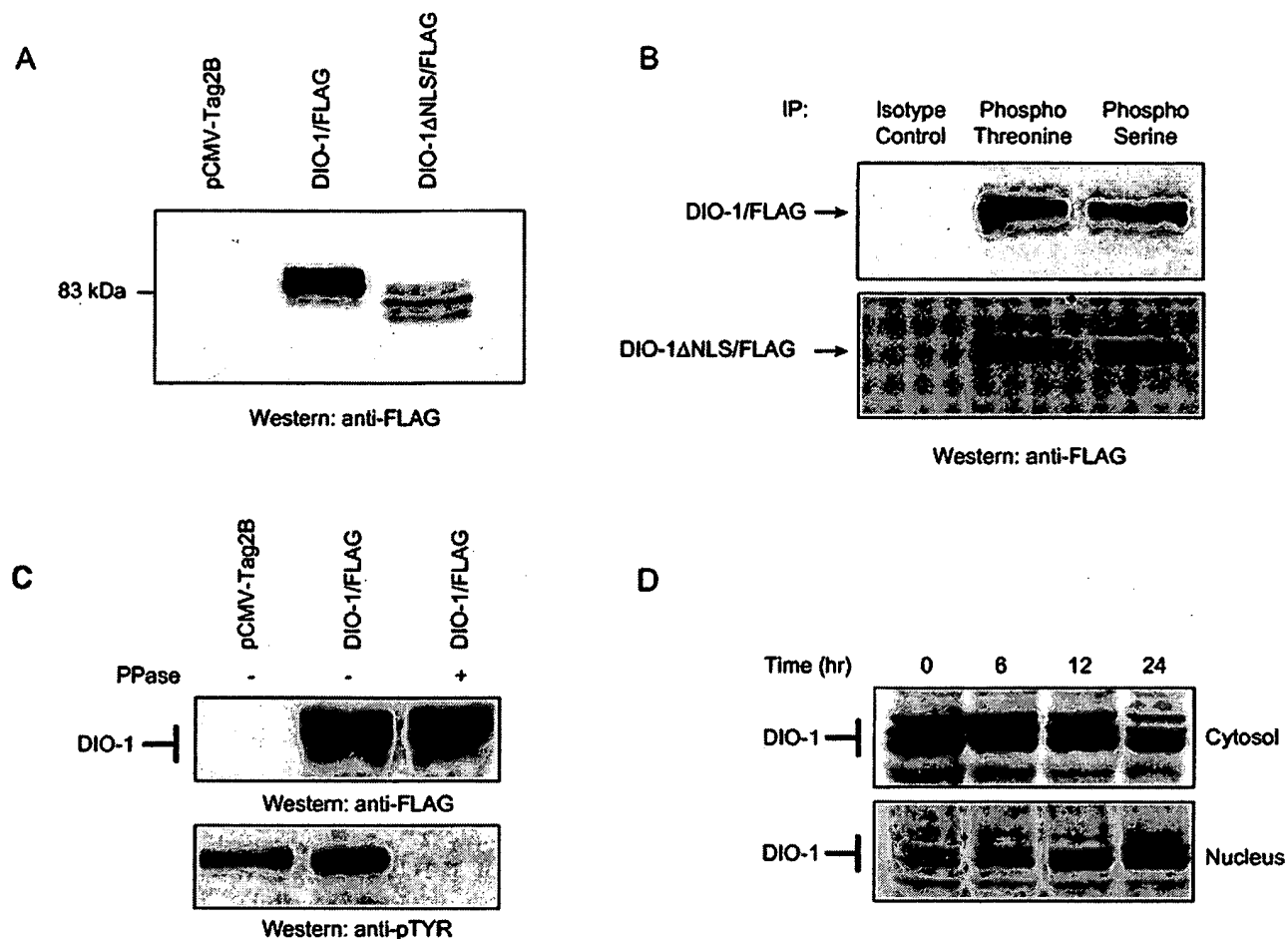


FIG. 4. DIO-1 is present in several forms with distinct subcellular distribution. (A) Western blot of lysates from 293T cells transfected with empty vector (pCMV-Tag2B), Flag-tagged DIO-1, or Flag-tagged DIO-1ΔNLS. The membrane was blotted with anti-Flag antibody. A representative result of five independent experiments is shown. Note the lower apparent molecular size of the deletion mutant and the three-band pattern. (B) 293T cells were transiently transfected with the indicated Flag-tagged constructs. Lysates were immunoprecipitated with antiphosphothreonine, antiphosphoserine, or an irrelevant control antibody and then blotted with anti-Flag monoclonal antibody. Only the upper and middle bands were detected. (C) 293T cells were transiently transfected with Flag-tagged DIO-1. Untreated or λ -phosphatase-treated lysates were separated by SDS-PAGE and then blotted with anti-Flag monoclonal antibody. Phosphatase treatment did not cause a mobility shift (upper panel). Dephosphorylation of total cellular proteins was verified by blotting with antiphosphotyrosine antibody (lower panel). (D) FL5.12 cells deprived of IL-3 for the times indicated were separated into cytosolic and nuclear fractions (Materials and Methods). Extracts were separated by SDS-PAGE and analyzed by Western blotting with the anti-DIO-1 antibody.

blotting with an anti-Flag antibody showed that DIO-1/Flag coimmunoprecipitated with DIO-1/Myc, whereas negative controls gave no bands (Fig. 3B). The amount of coprecipitated material was distributed equally among the three bands observed. To verify this interaction, we performed reciprocal experiments with anti-Flag to immunoprecipitate DIO-1/Flag, followed by blotting with anti-Myc. Concurring with the reverse experiment, DIO-1/Myc coimmunoprecipitated specifically with DIO-1/Flag (Fig. 3B). Similar experiments with DIO-1/Myc and DIO-1ΔNLS/Flag showed that both constructs coimmunoprecipitated (Fig. 3C), as confirmed by the reciprocal experiment (not shown). These results strongly suggest that DIO-1 homo-oligomerizes and that deletion of both NLS regions and their interspace does not affect this interaction. In addition, the C-terminal end of the protein is not needed for oligomerization, as glutathione *S*-transferase fusions lacking

the terminal 86 amino acids interacted with endogenous DIO-1 (not shown). The exact oligomerization site nonetheless remains to be determined. Based on computer predictions, the lysine-rich region, which resembles part of the *c-myc* dimerization site, may contribute to DIO-1 oligomerization; experiments are under way to analyze this possibility.

DIO-1 is present in multiple forms with distinct subcellular localizations. Triplet banding in Western blot, rather than a single band, may be produced by different protein phosphorylation states. To study this, Flag-tagged DIO-1 and DIO-1ΔNLS were transiently transfected in 293T cells and immunoprecipitated with antiphosphoserine, antiphosphothreonine, and antityrosine antibodies. Expression of both constructs showed the predicted three-band pattern (Fig. 4A), although only the two upper bands immunoprecipitated with antiphosphoserine and antiphosphothreonine (Fig. 4B). The lowest

band was absent, suggesting that it corresponds to a protein that is not phosphorylated on serine/threonine, whereas the two upper bands appeared to correspond to phosphorylated forms. Antiphosphotyrosine antibodies did not immunoprecipitate DIO-1 (not shown). Phosphatase treatment of cell extracts did not result in the loss of the multiple bands (Fig. 4C), indicating that the mobility shift was not caused by phosphorylation alone. These results nonetheless show that DIO-1 is present in multiple forms that differ in electrophoretic mobility. Of these, the larger forms are phosphorylated on serine/threonine residues.

To determine the role of the different DIO-1 forms in apoptosis, we examined their subcellular distribution and appearance under apoptotic conditions. Apoptosis was induced in FL5.12 cells by IL-3 withdrawal. Samples were taken at several time points, and the cytosolic and nuclear fractions were separated by centrifugation, resolved in SDS-PAGE, and analyzed in Western blots with the anti-DIO-1 antibody (Fig. 4D). Healthy cells (lanes labeled 0 h) showed higher DIO-1 protein levels in the cytosol than in the nucleus, as observed in the confocal images of MEF(10.1)Val5MycER cells; the three bands were present in the cytosolic fraction, whereas the upper band was nearly absent in the nucleus. With time, more cells entered apoptosis, and a progressive decrease was observed in the upper and middle cytosolic bands. At the same time, the nuclear fraction showed a clear increase in the lower band and a decrease in the middle band. These results suggest that the cytosolic form of DIO-1 is phosphorylated on serine/threonine and is predominant in healthy cells, whereas the unphosphorylated nuclear form is found under apoptotic conditions.

DIO-1 overexpression upregulates procaspase levels, leading to increased caspase activity. As discussed above, several lines of evidence suggest that nuclear translocation of DIO-1 is a step that activates the apoptotic machinery. Although the exact details of the programmed cell death pathways remain to be fully determined, the essential role of caspases at various stages of the apoptotic process has been established (3, 4, 38). The majority of apoptotic stimuli that signal through a pathway engage the common cell death machinery at the caspase level. We thus explored whether DIO-1 is also associated with caspase activation by examining procaspase levels and activity after transient expression of DIO-1 in FL5.12 cells.

Cells were initially treated with z-VAD-fmk to block proteolytic processing of the procaspases, facilitating accurate protein measurement in Western blot. Procaspases 3 and 9 were upregulated in wild-type cells induced to undergo apoptosis by IL-3 starvation. Similarly, DIO-1-transfected cells showed an increase in both proteins in the presence of IL-3, whereas transfection of the empty vector had no effect (Fig. 5A). In a fluorescence assay, protein lysates from cells not treated with caspase inhibitors were assayed for caspase activity. The previously observed increase in procaspase levels correlated with mature caspase activity (Fig. 5B). Caspase 3 showed an increase in activity following IL-3 starvation or DIO-1 expression compared to wild-type or mock-transfected cells. Caspases 6 and 9 were also activated, whereas caspase 2 showed lower activation levels. Caspase 8 was not implicated in IL-3-induced apoptosis and showed no variation after DIO-1 overexpression (not shown).

DIO-1ΔNLS is a dominant negative mutant that protects

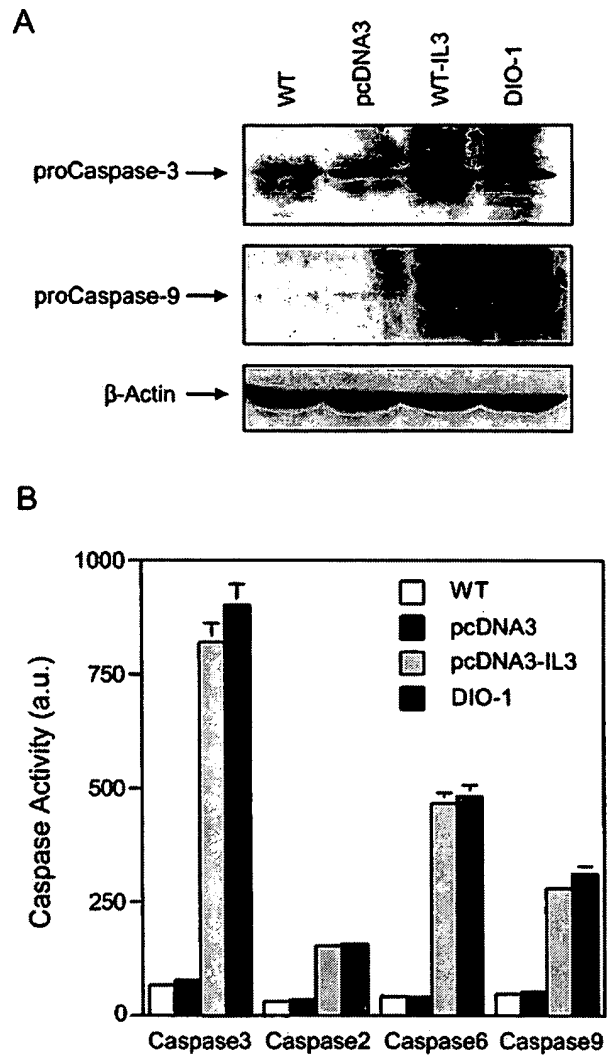


FIG. 5. DIO-1 upregulates and increases activation of caspases. (A) DIO-1 overexpression upregulates procaspase levels. FL5.12 cells were cultured in the presence of IL-3 (WT) or IL-3-starved for 24 h (WT-IL3). A plasmid vector (pcDNA3) or a DIO-1-expressing construct (DIO-1) were transiently transfected into FL5.12 cells and analyzed 24 h posttransfection. All cells were incubated with z-VAD-fmk (100 μ M) to block proteolytic processing of the procaspase, facilitating accurate quantitation of protein levels. Procaspase 3 and 9 levels were analyzed in Western blots with anti-caspase 3 (upper panel) or anti-caspase 9 antibodies (middle panel). Loading was controlled with β -actin (lower panel). (B) Conditions as for panel A, but apoptosis was induced by IL-3 removal in pcDNA3-transiently transfected FL5.12 cells. Cells were cultured in the absence of z-VAD-fmk to measure caspase activity. Caspase 3-like, caspase 2, caspase 6, and caspase 9 activities were determined by fluorescence emission of the cleaved substrates (Materials and Methods). Data are given as the mean \pm standard deviation for at least three independent experiments.

cells from apoptosis. To confirm that DIO-1 upregulates procaspases after its translocation to the nucleus, we performed similar experiments with the NLS deletion mutant, predicting failure to upregulate caspases due to its inability to translocate to the nucleus. We generated FL5.12 cells stably expressing DIO-1ΔNLS as well as a control bearing the empty vector. IL-3-starved empty vector cells showed procaspase 3 and 9 upregu-

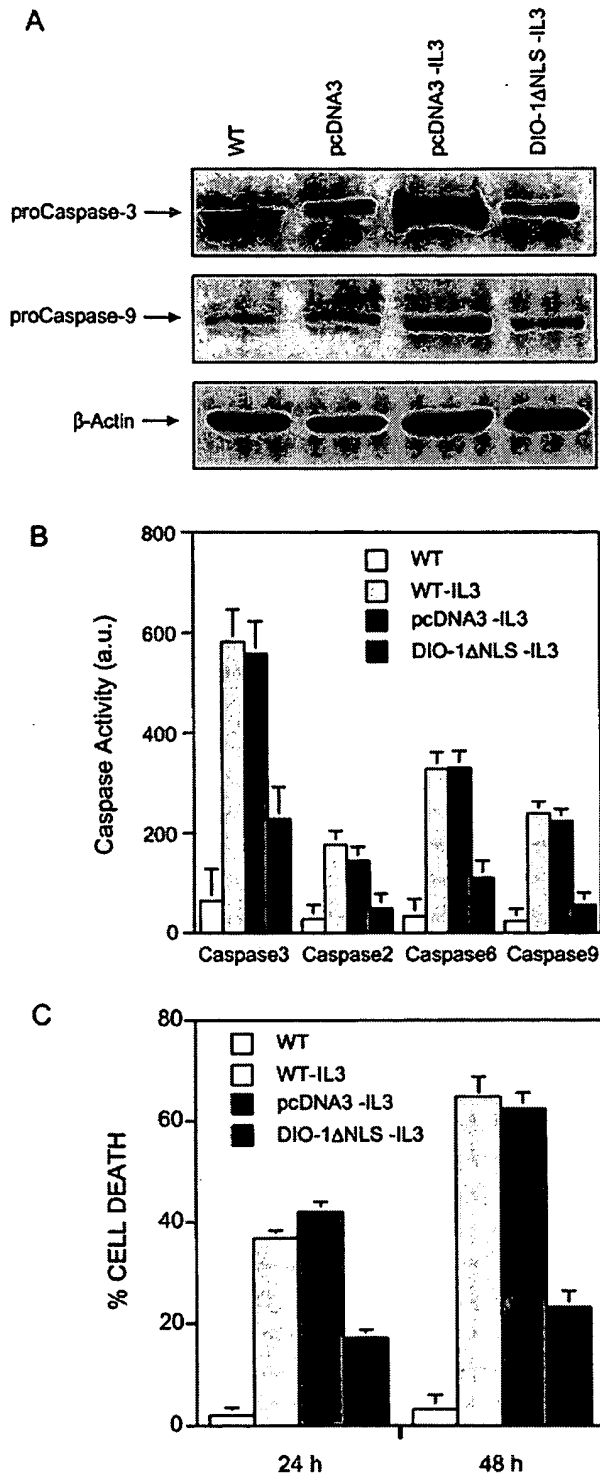


FIG. 6. DIO-1ΔNLS mutant is unable to upregulate and activate caspases. (A) FL5.12 cells were untreated (WT) or stably transfected with an empty vector (pcDNA3) or a DIO-1ΔNLS-expressing construct. Where indicated, IL-3 was removed from culture medium, and analysis was performed after 24 h. All cells were cultured in the presence of z-VAD-fmk (100 μM). Lysates were resolved by SDS-PAGE, followed by Western blotting with anti-caspase 3 (upper panel) or anti-caspase 9 (middle panel) antibodies. Loading was controlled with β-actin (lower panel). (B) Analysis of caspase activation. Samples

lation, whereas IL-3-starved cells expressing DIO-1ΔNLS did not upregulate procaspase levels (Fig. 6A). In addition, caspase activity in IL-3-starved DIO-1ΔNLS-expressing cells was clearly below the levels observed in DIO-1-transfected cells (Fig. 6B; compare to Fig. 5B). These low activity levels remained constant even after 48 h of IL-3 deprivation, when more than 60% of wild-type cells were apoptotic (not shown). The mutation thus failed to alter basal caspase levels. Taken together, these data suggest that DIO-1 translocation to the nucleus is essential to induce upregulation of several procaspases, to increase their activity, and to trigger the apoptotic pathway.

Given that the NLS mutation does not alter caspase levels, we tested whether it prevents apoptosis. FL5.12 wild-type cells were IL-3 starved, and apoptosis was measured by propidium iodide staining at 24 and 48 h postinduction (Fig. 6C). The cells underwent apoptotic cell death that increased with time, and similar results were obtained in FL5.12 pcDNA3 cells after IL-3 withdrawal. When FL5.12 cells stably expressing DIO-1ΔNLS (FL5.12 DIO-1ΔNLS) were IL-3 starved, we observed protection from apoptosis even after 48 h without the survival factor, with a reduction in the percentage of apoptotic cells of approximately 50% at 24 h and 66% at 48 h compared to cells expressing the empty vector. This behavior corresponds to a dominant negative mutation that is able to block the apoptotic signal transmitted by the wild-type form.

DISCUSSION

We report that DIO-1 translocation from the cytoplasm to the nucleus is an important early event in activating the apoptotic machinery. DIO-1 is present in the cell in multiple forms, which can be distinguished on the basis of their electrophoretic mobilities and their distinct subcellular localizations. We previously showed that DIO-1 mRNA and protein levels were upregulated by serum withdrawal from MEF(10.1)Val5MycER cells independently of p53-induced apoptosis (9). Here we show that, in the same cell system and with the same apoptotic stimulus, the DIO-1 gene product translocated to the nuclear compartment, whereas p53-induced cell death did not provoke alterations in its subcellular localization. The DIO-1 mutant lacking both NLSs (DIO-1ΔNLS) was unable to translocate to the nucleus or to trigger apoptosis, even in the presence of physiological death signals, and prevented IL-3 deprivation-induced cell death. The obser-

were collected from FL5.12 wild-type (WT) cells cultured in the presence or absence of IL-3 and from the indicated stable FL5.12 cell lines in the absence of IL-3. Caspase activity was measured as in Fig. 5B. Results are expressed as the mean ± standard deviation for at least three independent experiments. (C) DIO-1ΔNLS is a dominant negative mutant that protects cells from growth factor deprivation-induced apoptosis. FL5.12 wild-type cells (WT) and the FL5.12pcDNA3, and FL5.12DIO-1ΔNLS stable cell lines were induced to undergo apoptosis by IL-3 removal. Cells were collected at the times indicated, permeabilized, and propidium iodide stained (Materials and Methods). Apoptosis corresponds to the amount of fragmented DNA in the hypodiploid sub-G₀/G₁ peak of the cell cycle. Values are expressed as percentages and represent the mean ± standard deviation for at least three independent experiments.

vation that DIO-1 but not DIO-1ΔNLS overexpression up-regulated procaspase 3 and 9 levels and increased the activity of their mature forms establishes a link between the increase in DIO-1 levels and apoptosis induction (9). Although transcriptional activation by DIO-1 remains to be demonstrated, the need for nuclear translocation suggests that DIO-1 acts through the induction of caspase promoters rather than exerting a direct effect on cytoplasmic caspases. These findings are consistent with earlier studies reporting that transcriptional activation of caspases may be an important regulatory mechanism in programmed cell death (6, 12, 22, 29, 40).

One important model for caspase 9 activation involves its recruitment to Apaf-1 in the presence of ATP or dATP, following cytochrome *c* release from mitochondria (19, 42). Other authors propose that caspase 9 is activated and apoptosis can take place in the absence of cytochrome *c* (5, 10, 20, 32) after overexpression of the adaptor molecule Apaf-1 (16, 28), Nod-1 (14), TMS-1 (26), or CED-4 (35, 41). Furthermore, Apaf-1 mutants lacking the WD-40 repeats (WDR) constitutively self-associate and activate procaspase 9 independently of cytochrome *c* and dATP (13, 37). The *Caenorhabditis elegans* Apaf-1 homolog CED-4 lacks the WDR, implying that it may constitutively activate the procaspase 9 homolog CED-3 and suggesting that cytochrome *c* may not be required for CED-4-mediated CED-3 activation.

In our system, apoptosis induction via a DIO-1-triggered increase in procaspase 9 levels concurs with previous reports that procaspase 9 overexpression in vivo results in cell death, overriding the need for cytosolic cytochrome *c* (2, 14, 37). We observed that in MEF(10.1)Val5MycER and FL5.12 cells induced to apoptosis as well as in DIO-1-transfected cells, cytochrome *c* release was preceded by DIO-1 nuclear translocation and caspase upregulation (not shown). Caspase 9 activation is thus mediated by dimerization, and cytochrome *c*-induced recruitment by Apaf-1 creates high local caspase 9 concentrations that allow dimer-induced activation (31). This explains the caspase 9 activation observed prior to cytochrome *c* release from mitochondria.

Change in subcellular distribution is an important regulatory event for many proteins involved in apoptosis, cell cycle, or transcriptional regulation. Here we show that DIO-1 also changes its localization early in apoptosis induction and that this change is accompanied by an electrophoretic mobility shift. Nonetheless, the exact nature of the signal leading to these changes remains to be established. Coprecipitation of differentially tagged proteins showed that DIO-1 forms homo-oligomers in vivo. As homo-oligomers were detected for all forms, the oligomerization state is unlikely to differ following DIO-1 translocation to the nucleus. This has also been found for p53, which appears to be transported across the nuclear membrane in a tetrameric form (11). Proteolytic processing can also be ruled out as a regulatory mechanism, since all forms were detected with tags on either end of the protein. Although only the forms with lower electrophoretic mobility appeared to be phosphorylated, phosphorylation alone is not the basis of the mobility change. Additional modifications may thus be needed for the change in DIO-1 localization. In a similar case, MDM-2-mediated nuclear export of p53 depends on multiple signals that include the DNA-binding domain, conformational change, and C-terminal ubiquitination (11,

24); ubiquitinated p53 is subsequently degraded by proteasomes in the cytosol. DIO-1 localization may be regulated in a similar fashion. DIO-1 would thus be continuously modified and exported from the nucleus in healthy cells, appearing as cytosolic localization. In apoptotic cells, loss of the export signal would result in a net accumulation of the unmodified product in the nucleus.

DIO-1-mediated apoptosis requires caspase activation. In these experiments, neither procaspase upregulation nor caspase activation was detected after DIO-1ΔNLS overexpression, indicating that this mutant acts in a dominant negative manner, since it inhibits IL-3 withdrawal-induced apoptosis. This allows us to propose a model that explains the mechanism of DIO-1 activation and induction of cell death. In healthy cells, the DIO-1 transcript and protein are expressed at low basal levels, and the protein is found in the cytosol. Following an appropriate apoptotic stimulus, such as IL-3 starvation or *c-myc* induction in serum-free conditions, DIO-1 translocates to the nucleus before the appearance of any classical indicators of apoptotic machinery activation, such as caspase activation, alteration of cell membrane polarity, nuclear disruption, or DNA laddering. This indicates that DIO-1 activation is a very early step in apoptosis induction.

In our model, the presence of DIO-1 in the nucleus leads to an increase in procaspase 3 and 9 levels, resulting in caspase 9 activation. Activated caspase 9 can then activate procaspase 3. The processing of the large amounts of procaspase 3 gives rise to rapid accumulation of mature caspase 3, which acts as another amplification step due to caspase 3 feedback onto procaspase 9 Asp-330 (37). Subsequent cytochrome *c* release from mitochondria would induce Apaf-1 oligomerization, amplifying the apoptotic signal. The DIO-1ΔNLS mutant could form stable oligomers with wild-type DIO-1 and block nuclear translocation of the entire complex, preventing DIO-1-mediated gene upregulation and inhibiting the cell death program.

ACKNOWLEDGMENTS

We thank B. B. Wolf, D. R. Green, T. W. Mak, and R. Hakem for generous gifts of reagents, A. Ruiz-Vela for excellent and continuous advice, and A. Fütterer and M. Torres, A. Ruiz-Vela, K. van Wely, and M. Campanero for critical reading of the manuscript. We also thank I. López-Vidriero and M. C. Moreno-Ortiz for help with flow cytometry, all technical members of the department who aided with cell culture and general reagents, and C. Mark for editorial assistance.

D.G.D. is the recipient of a fellowship from the Spanish Ministerio de Educación y Ciencia. This work was supported by grants from the Ministerio de Ciencia y Tecnología and the European Union (QLG1-CT-2001-01536). The Department of Immunology and Oncology was founded and is supported by the Spanish Council for Scientific Research (CSIC) and the Pharmacia Corporation.

REFERENCES

1. Alnemri, E. S., D. J. Livingston, D. W. Nicholson, G. Salvesen, N. A. Thornberry, W. W. Wong, and J. Yuan. 1996. Human ICE/CED-3 protease nomenclature. *Cell* 87:171.
2. Bertin, J., W. J. Nir, C. M. Fischer, O. V. Tayber, P. R. Errada, J. R. Grant, J. J. Kelly, M. L. Gosselin, K. E. Robison, G. H. Wong, M. A. Glucksmann, and P. S. DiStefano. 1999. Human CARD4 protein is a novel CED-4/Apaf-1 cell death family member that activates NF- κ B. *J. Biol. Chem.* 274:12955–12958.
3. Boldin, M. P., T. M. Goncharov, Y. V. Goltsev, and D. Wallach. 1996. Involvement of MACH, a novel MORT1/FADD-interacting protease, in Fas/APO-1- and TNF receptor-induced cell death. *Cell* 85:803–815.
4. Budihardjo, I., H. Oliver, M. Lutter, X. Luo, and X. Wang. 1999. Biochemical pathways of caspase activation during apoptosis. *Annu. Rev. Cell Dev. Biol.* 15:269–290.

5. Chauhan, D., T. Hideshima, S. Rosen, J. C. Reed, S. Kharbanda, and K. C. Anderson. 2001. Apaf-1/cytochrome c-independent and Smac-dependent induction of apoptosis in multiple myeloma (MM) cells. *J. Biol. Chem.* 276: 24453–24456.
6. Dai, C., and S. B. Krantz. 1999. Interferon gamma induces upregulation and activation of caspases 1, 3, and 8 to produce apoptosis in human erythroid progenitor cells. *Blood* 93:3309–3316.
7. Earnshaw, W. C., L. M. Martins, and S. H. Kaufmann. 1999. Mammalian caspases: structure, activation, substrates, and functions during apoptosis. *Annu. Rev. Biochem.* 68:383–424.
8. Ellis, R. E., J. Y. Yuan, and H. R. Horvitz. 1991. Mechanisms and functions of cell death. *Annu. Rev. Cell Biol.* 7:663–698.
9. Garcia-Domingo, D., E. Leonardo, A. Grandien, P. Martinez, J. P. Albar, J. C. Izpisua-Belmonte, and C. Martinez-A. 1999. DIO-1 is a gene involved in onset of apoptosis *in vitro*, whose misexpression disrupts limb development. *Proc. Natl. Acad. Sci. USA* 96:7992–7997.
10. Gross, A., J. Jockel, M. C. Wei, and S. J. Korsmeyer. 1998. Enforced dimerization of BAX results in its translocation, mitochondrial dysfunction and apoptosis. *EMBO J.* 17:3878–3885.
11. Gu, J., L. Nie, D. Wiedersheim, and Z. M. Yuan. 2001. Identification of p53 sequence elements that are required for MDM2-mediated nuclear export. *Mol. Cell. Biol.* 21:8533–8546.
12. Gupta, S., V. Radha, Y. Furukawa, and G. Swarup. 2001. Direct transcriptional activation of human caspase-1 by tumor suppressor p53. *J. Biol. Chem.* 276:10585–10588.
13. Hu, Y., M. A. Benedict, L. Ding, and G. Nuñez. 1999. Role of cytochrome c and dATP/ATP hydrolysis in Apaf-1-mediated caspase-9 activation and apoptosis. *EMBO J.* 18:3586–3595.
14. Inohara, N., T. Koseki, L. del Peso, Y. Hu, C. Yee, S. Chen, R. Carrio, J. Merino, D. Liu, J. Ni, and G. Nuñez. 1999. Nod1, an Apaf-1-like activator of caspase-9 and nuclear factor- κ B. *J. Biol. Chem.* 274:14560–14567.
15. Jacobson, M. D., M. Weil, and M. C. Raff. 1997. Programmed cell death in animal development. *Cell* 88:347–354.
16. Kamarajan, P., N. K. Sun, C. L. Sun, and C. C. Chao. 2001. Apaf-1 overexpression partially overcomes apoptotic resistance in a cisplatin-selected HeLa cell line. *FEBS Lett.* 505:206–212.
17. Kerr, J. F., A. H. Wyllie, and A. R. Currie. 1972. Apoptosis: a basic biological phenomenon with wide-ranging implications in tissue kinetics. *Br. J. Cancer* 26:239–257.
18. Li, H., H. Zhu, C. J. Xu, and J. Yuan. 1998. Cleavage of BID by caspase 8 mediates the mitochondrial damage in the Fas pathway of apoptosis. *Cell* 94:491–501.
19. Li, P., D. Nijhawan, I. Budihardjo, S. M. Srinivasula, M. Ahmad, E. S. Alnemri, and X. Wang. 1997. Cytochrome c and dATP-dependent formation of Apaf-1/caspase-9 complex initiates an apoptotic protease cascade. *Cell* 91:479–489.
20. Li, P. F., R. Dietz, and R. von Harsdorf. 1999. p53 regulates mitochondrial membrane potential through reactive oxygen species and induces cytochrome c-independent apoptosis blocked by Bcl-2. *EMBO J.* 18:6027–6036.
21. Liang, P., and A. B. Pardee. 1992. Differential display of eukaryotic messenger RNA by means of the polymerase chain reaction. *Science* 257:967–971.
22. Liu, W., G. Wang, and A. G. Yakovlev. 2002. Identification and functional analysis of the rat caspase-3 gene promoter. *J. Biol. Chem.* 277:8273–8278.
23. Liu, X., C. N. Kim, J. Yang, R. Jemmerson, and X. Wang. 1996. Induction of apoptotic program in cell-free extracts: requirement for dATP and cytochrome c. *Cell* 86:147–157.
24. Lohrum, M. A., D. B. Woods, R. L. Ludwig, E. Balint, and K. H. Vousden. 2001. C-terminal ubiquitination of p53 contributes to nuclear export. *Mol. Cell. Biol.* 21:8521–8532.
25. Luo, X., I. Budihardjo, H. Zou, C. Slaughter, and X. Wang. 1998. Bid, a Bcl2 interacting protein, mediates cytochrome c release from mitochondria in response to activation of cell surface death receptors. *Cell* 94:481–490.
26. McConnell, B. B., and P. M. Vertino. 2000. Activation of a caspase-9-mediated apoptotic pathway by subcellular redistribution of the novel caspase recruitment domain protein TMS1. *Cancer Res.* 60:6243–6247.
27. Muzio, M., A. M. Chinnaiyan, F. C. Kischkel, K. O'Rourke, A. Shevchenko, J. Ni, C. Scaffidi, J. D. Bretz, M. Zhang, R. Gentz, M. Mann, P. H. Kramer, M. E. Peter, and V. M. Dixit. 1996. FLICE, a novel FADD-homologous ICE/CED-3-like protease, is recruited to the CD95 (Fas/APO-1) death-inducing signaling complex. *Cell* 85:817–827.
28. Perkins, C., C. N. Kim, G. Fang, and K. N. Bhalla. 1998. Overexpression of Apaf-1 promotes apoptosis of untreated and paclitaxel- or etoposide-treated HL-60 cells. *Cancer Res.* 58:4561–4566.
29. Pohl, D., P. Bittigau, M. J. Ishimaru, D. Stadthaus, C. Hubner, J. W. Olney, L. Turski, and C. Ikonomidou. 1999. N-Methyl-D-aspartate antagonists and apoptotic cell death triggered by head trauma in developing rat brain. *Proc. Natl. Acad. Sci. USA* 96:2508–2513.
30. Raff, M. 1998. Cell suicide for beginners. *Nature* 396:119–122.
31. Renatus, M., H. R. Stennicke, F. L. Scott, R. C. Liddington, and G. S. Salvesen. 2001. Dimer formation drives the activation of the cell death protease caspase 9. *Proc. Natl. Acad. Sci. USA* 98:14250–14255.
32. Ruiz-Vela, A., G. Gonzalez de Buitrago, and C. Martinez-A. 1999. Implication of calpain in caspase activation during B cell clonal deletion. *EMBO J.* 18:4988–4998.
33. Salvesen, G. S., and V. M. Dixit. 1999. Caspase activation: the induced-proximity model. *Proc. Natl. Acad. Sci. USA* 96:10964–10967.
34. Salvesen, G. S., and V. M. Dixit. 1997. Caspases: intracellular signaling by proteolysis. *Cell* 91:443–446.
35. Shaham, S., and H. R. Horvitz. 1996. Developing *Caenorhabditis elegans* neurons may contain both cell-death protective and killer activities. *Genes Dev.* 10:578–591.
36. Smith, P. K., R. I. Krohn, G. T. Hermanson, A. K. Mallia, F. H. Gartner, M. D. Provenzano, E. K. Fujimoto, N. M. Goeke, B. J. Olson, and D. C. Klenk. 1985. Measurement of protein with bicinchoninic acid. *Anal. Biochem.* 150:76–85.
37. Srinivasula, S. M., M. Ahmad, T. Fernandes-Alnemri, and E. S. Alnemri. 1998. Autoactivation of procaspase-9 by Apaf-1-mediated oligomerization. *Mol. Cell* 1:949–957.
38. Thornberry, N. A., and Y. Lazebnik. 1998. Caspases: enemies within. *Science* 281:1312–1316.
39. Wolf, B. B., J. C. Goldstein, H. R. Stennicke, H. Beere, G. P. Amarante-Mendes, G. S. Salvesen, and D. R. Green. 1999. Calpain functions in a caspase-independent manner to promote apoptosis-like events during platelet activation. *Blood* 94:1683–1692.
40. Yakovlev, A. G., K. Ota, G. Wang, V. Movsesyan, W. L. Bao, K. Yoshihara, and A. I. Faden. 2001. Differential expression of apoptotic protease-activating factor-1 and caspase-3 genes and susceptibility to apoptosis during brain development and after traumatic brain injury. *J. Neurosci.* 21:7439–7446.
41. Yuan, J., and H. R. Horvitz. 1992. The *Caenorhabditis elegans* cell death gene CED-4 encodes a novel protein and is expressed during the period of extensive programmed cell death. *Development* 116:309–320.
42. Zou, H., W. J. Henzel, X. Liu, A. Lutschg, and X. Wang. 1997. Apaf-1, a human protein homologous to *C. elegans* CED-4, participates in cytochrome c-dependent activation of caspase-3. *Cell* 90:405–413.

Alignment of KIAA0333 (i.e. from Nagase *et al*) and DIO-1. The Nuclear Localisation Signal is underlined (co-ordinates 162-170 and 182-190)

KIAA0333	1
DIO-1	1	MDDKGHLSNEEAPKAIKPTSKEFRKTWGFRRTTIAKREGAGDTEADPSEQQPQHNLSLR
Consensus	1
KIAA0333	1
DIO-1	61	RSGRQPKRTERVEEFLTTVRRRGKKNVPVSLEDSSEPTSSTVTDVETASEGSVESSEIR
Consensus	1
KIAA0333	1
DIO-1	121	SGPVSDSLGKEHPASSEKAKGEEEEEDTSDSDSGLTLKEL <u>QNRLRRKRE</u> QEPVERSLRG
Consensus	1
KIAA0333	1 <u>ESK</u> LEGKAA
DIO-1	181	<u>SONRLRKKRR</u> REEDSAETGSVQIGSAEQDRPLCKQEPEASQGPVSQSETDDI <u>ENQ</u> LEGKAT
Consensus	1 <u>ENQ</u> LEGKAA
KIAA0333	10	<u>QDIKUEEP</u> GLGRPKPECEGYDPNALYCICRQPHNNRFMICCDRCEEFHGDVGVISEAR
DIO-1	241	<u>QGNTEENPRE</u> AGKPKPECEVYDPNALYCICRQPHNNRFMICCDRCEEFHGDVGVISEAR
Consensus	10	<u>QDNK#E#PR#</u> AGRPKPECEGYDPNALYCICRQPHNNRFMICCDRCEEFHGDVGVISEAR
KIAA0333	70	<u>GRLLRNGEDYICPNCTILQVQDETHSE</u> TADQQAQKWRPGDADGTDCTSIGTIEQKSSSED
DIO-1	301	<u>GRLLRNGEDYICPNCTILQVQDETNGSA</u> TNEQDSGCRSVGADGTDCTSIGTIEQKSGED
Consensus	67	<u>GRLLRNGEDYICPNCTILQVQDETNGEA</u> ##Q#AGCRPGDADGTDCTSIGTIEQKSGED
KIAA0333	130	<u>QGIKGRIEKAANPSGKKKLKIFQP</u> GPGPVPTQLPVLWQVLEIAVSRISISAFTLLHCISCK
DIO-1	361	<u>QGIKGRIEKAANPSGKKKLKIFQP</u>
Consensus	123	<u>QGIKGRIEKAANPSGKKKLKIFQP</u>
KIAA0333	190	<u>VTEAPGAS</u> SKCIGPGCCHVAQPDSVYCSNDCILKHAATMRFLLSSGKEQKPKPKMKMKMP
DIO-1	385	<u>VTEAPGAPKCIGPGC</u> SSVAQPDSVYCSNDCILKHAATMRFLLSSGKEQKTKPKKTKPK
Consensus	147	<u>VTEAPGAPKCIGPGCCHVAQPDSVYCSNDCILKHAATMRFLLSSGKEQKPKPKMKMKMP</u>
KIAA0333	250	<u>EKPSLPKCGAQAGIKISSVHKRP</u> PAPEKKETTIVKKA>VVPARSEALGKEAACESSTPSWAS
DIO-1	445	<u>EKFSLPKCSVQV</u> GIKISSVHKRLASEKRENPVKK.VMLASRSETSGKEAACESSTPSWAS
Consensus	206	<u>EKFSLPKCGAQAGIKISSVHKRLA</u> PEKRENPVKK.VMLAARSEALGKEAACESSTPSWAS
KIAA0333	310	<u>DHNYNAVKPEKTAAP</u> ...SPSLLYKSTKEDRRSEKAAATAASKKTAPPGSTVQKQP..A
DIO-1	504	<u>DHNYNAVKPEKPEKPTAL</u> SPILLSKCTYHPKAGFPGPSHLLGGCLGLSRTIVLGVVLIV
Consensus	265	<u>DHNYNAVKPEKPAAP</u> ...SPSLLSKCTKEDRAGEEGAAHAAGCLGAPRGRTLQKQP..A
KIAA0333	365	<u>PRNLMPKSSSEANVAAATPAIKKPP</u> SGFKCTIPKRPWLSATPSSGASAARQAGPAPAAAT
DIO-1	564	<u>ASSSLPARSRMODASGPQVE</u> IPSLWSLSGWEEKSCVGLMLEATSYFSFRPW.....
Consensus	320	<u>ARNLLPARSR</u> ##AAAAQPAIKKLPSGFGGFIKKRPGLMAEATSGASAARQ.....
KIAA0333	425	AASKKFPGSAAALVGAVRKPVVPSVPMASAPAGRLGAMSAAPSQPNSQIRQNIRSLKEIL
DIO-1	
Consensus	

KIAA0333	485	WKRVDSDDDLIMTENEVGKIALHIEKEMFNLFQVTDNRYKSKYRSIMFNLKDPKNQGLFH
DIO-1	
Consensus	
KIAA0333	545	RVLREEISLAKLVRLKPEELVSKELSTWKERPARSVMESRTKLHNESKKTAPRQEAI PDL
DIO-1	
Consensus	
KIAA0333	605	EDSPPVSDSEEQQESARAVPEKSTAPLLDVFSSMLKDTTSQHRAHLFDLNCKICTGQVPS
DIO-1	
Consensus	
KIAA0333	665	AEDEPAPKKQKLSASVKKEDLKSKHDSSAPDPAPDSADEVMPEAVPEVASEPGLESASHP
DIO-1	
Consensus	
KIAA0333	725	NVDRTYFPGPPGDGHPEPSPLEDLSPCPASCGSGVTTTVTVSGRDPRTAPSSSCTAVASA
DIO-1	
Consensus	
KIAA0333	785	ASRPDSTHMVEARQDVPKPVLTSMVPKSILAKPSSSPDPRYLSVPPSPNISTSESRSPP
DIO-1	
Consensus	
KIAA0333	845	EGDTTLFLSRLSTIWKGFINMQSVAKFVTKAYPVSGCFDYLSDEL PDIHIGGRIAPKTV
DIO-1	
Consensus	
KIAA0333	905	WDYVGKLKSSVSKELCLIRFHPATEEEEVAYISLYSYFSSRGRFGVVANNNRHVKDLYLI
DIO-1	
Consensus	
KIAA0333	965	PLSAQDPVPSKLLPFEGPGKRRLSGWR
DIO-1	
Consensus	

**This Page is Inserted by IFW Indexing and Scanning
Operations and is not part of the Official Record**

BEST AVAILABLE IMAGES

Defective images within this document are accurate representations of the original documents submitted by the applicant.

Defects in the images include but are not limited to the items checked:

☒ **BLACK BORDERS**

☐ **IMAGE CUT OFF AT TOP, BOTTOM OR SIDES**

☐ **FADED TEXT OR DRAWING**

☒ **BLURRED OR ILLEGIBLE TEXT OR DRAWING**

☐ **SKEWED/SLANTED IMAGES**

☒ **COLOR OR BLACK AND WHITE PHOTOGRAPHS**

☐ **GRAY SCALE DOCUMENTS**

☐ **LINES OR MARKS ON ORIGINAL DOCUMENT**

☒ **REFERENCE(S) OR EXHIBIT(S) SUBMITTED ARE POOR QUALITY**

☐ **OTHER:** _____

IMAGES ARE BEST AVAILABLE COPY.

As rescanning these documents will not correct the image problems checked, please do not report these problems to the IFW Image Problem Mailbox.